Tropical Cyclone Tracks and the Subtropical High Pressure System in the North-Atlantic in a 400-year Climate Simulation

Master's Thesis

Faculty of Science
University of Bern

presented by

Sina Lenggenhager

2013

Supervisor:
Prof. Dr. Olivia Romppainen-Martius

Institute of Geography and
Oeschger Centre for Climate Change Research, University of Bern

Co-Supervisor:
Prof. Dr. Stefan Brönnimann

Institute of Geography, University of Bern

Advisor:
Dr. Paul Della-Marta

PartnerRe, Zürich

Abstract

Tropical cyclones and their behaviour in a changing climate are still strongly debated in the scientific community. This study investigates the impact of long-term variability of the North-Atlantic subtropical high pressure system (NASH) on tropical cyclone tracks. As a basis a 400-year climate simulation data set was used, that consists of 30 model runs of the ECHAM5.4 model. It is investigated for its ability to reproduce the North-Atlantic circulation patterns by comparing it to ERA-Interim reanalysis data. Then, artificial tropical cyclone tracks were simulated with help of a beta-and-advection model. With that, three simulations were carried out, each one comparing tracks generated in a period with a strong NASH with tracks generated in a period with a weak one. It is shown that a strong NASH tends to move the TCs faster and causes them to recurve more when developing in the western part of the main development region, while they tend to move more straight crossing the tropical North-Atlantic when developing in the eastern part. Further it is shown that the influence of the July to October mean steering flow is much smaller than the influence of the genesis location. Thus, the third simulation, which simulated storm tracks in the periods between 1930-1959 and 1970-1999 on the date and location of the corresponding HURDAT observational data, did not show a clear sign regarding the influence of the steering flow on the tracks, because a substantial shift in genesis location was found.

Contents

Chapter 1

Introduction

Tropical cyclones (TCs) are among the most devastating weather systems. At maturity, winds of more than 90 m/s and diameters of 1000 km can occur (*AMS glossary*). If a TC makes landfall, it can have substantial socio-economic impacts. Storm surges, the high wind speeds and heavy rains can destroy entire regions. Mainly due to more people moving to the coast and an increase in wealth, the economic losses by TCs have been increasing over the past decades. This led to an increasing interest in both the reasons for this increase and the predictability of TCs in general. However, it is still an open question if and how global warming will influence TCs (Trenberth, 2005). Most of the studies agree that the total number of TCs is not likely to rise, but there are studies showing that intense TCs could become more frequent (Knutson et al., 2010). A lot of research has recently been conducted in this field, with most of the studies focusing on variability of TC intensities citep[i.e.][]Emanuel2005, Webster2005 or TC numbers (i.e. Landsea, 2007; Mann et al., 2009; Vecchi and Knutson, 2008). More prominent than the anthropogenic influence on is the influence of different climate modes on TC activity. El-Niño Southern Oscillation (ENSO), for example, is known to influence seasonal TC activity (i.e. Gray, 1984; Murakami and Wang, 2010) in the Atlantic. In El-Niño years the TC formation over the North-Atlantic is strongly reduced (i.e. Elsner, 2003; Murakami and Wang, 2010; Xie et al., 2005).

Compared to the large amount of research focusing on the change in intensity of TCs, there is only little research going on about the paths that they are taking (hereafter referred to as TC tracks). Nevertheless, TC tracks are more and more discussed in the scientific community. Especially for insurance and reinsurance companies, but also for the people living in vulnerable regions it is essential to know the mechanisms of the TC tracks. Unfortunately, as there is not enough observational data to assess the risk over a small area and the general circulation models have problems to resolve TCs accurately (Bengtsson et al., 2006; Camargo et al., 2004; Strachan et al., 2013), probabilistic risk models rely on artificially simulated TC tracks (Della-Marta and Prechtl, 2010). This is

where the present study sets in. We have a very large simulation data set that covers the last 400 years and has 30 different model runs, which means we have 12'000 years of simulated data. This data set offers the opportunity to produce thousands of simulated TC tracks that could help the regional risk assessment.

State of Research

Tropical cyclones are warm-core low pressure systems over the tropical or subtropical oceans and are, in contrast to extratropical cyclones, driven by latent heat release of the condensing water vapour (Fink and Speth, 1998). For a TC to develop, the following preconditions are needed: Sea temperatures of more than $26.5°$ C in the upper 60 m, little vertical wind shear (<10m/s) between the upper and the lower troposphere, a moist mid-troposphere, a strong enough Coriolis force (>5° latitude) and a preexisting disturbance (Fink and Speth, 1998). In the Atlantic these prerequisites are most often fulfilled in the region between $10°$ and $20°$ N.

But not only the genesis location is important for the TC tracks, but also the direction the TC is steered to (Colbert and Soden, 2012). The combination of these two processes leads to complex interactions of the large-scale atmospheric dynamics and the TC tracks. Different studies have shown that North-Atlantic modes, such as the North-Atlantic-Oscillation (NAO), the Atlantic Multidecadal Oscillation (AMO) and the Atlantic Meridional Mode (AMM) influence the TC tracks. Xie et al. (2005), for example, showed that a positive NAO index leads to an east-west gradient in the density of TC tracks in the North-Atlantic. A negative NAO tends to be associated with more TCs making landfall along the US East Coast. This is in accordance with the study of Kossin and Vimont (2007) that showed that positive AMM phases are associated with higher sea surface temperatures (SSTs), lower wind shear in the tropical North-Atlantic and higher TC numbers. This is most pronounced close to the equator (Kossin et al., 2010). Elsner (2003) suppose the NAO to influence the steering of the TC while ENSO impacts the genesis. They could further associate a low NAO with more TCs making landfall in the south-eastern US, and hypothesise the low NAO to be associated with a south-west shifted North-Atlantic subtropical high-pressure system (NASH). However, Colbert and Soden (2012) stated that the NAO only influences TCs that form outside the main development region (MDR).

One of the few studies that deal with the influence of the NASH on TC tracks was conducted by Colbert and Soden (2012). They subdivided cyclone tracks into three different types: "Straight moving", "recurving ocean" and "recurving landfall". They could show that a westward extension and a strengthening of the NASH falls together with more straight moving tracks, whereas a weakening of the NASH favours recurving ocean tracks, thus less TCs making landfall (Colbert and Soden, 2012). They

further associated this to both a shift in genesis location and a change in the steering flow. Their study was based on six-hourly data, reaching back to 1960.

In the same year Li et al. (2012) postulated a strengthening of the subtropical high pressure systems in a warming climate. However, the cause of the long-term variability in NASH as well as the impact of this variability on TCs is still poorly understood (Colbert and Soden, 2012; Li et al., 2012). In this study 400-year climate simulation data is used to improve the understanding of the long-term variability of the NASH and its influence on TC tracks. The following research questions are addressed:

- Are the Atlantic circulation patterns well represented in the CCC400 data?

- Is the CCC400 data suitable for simulating TC tracks?

- Is there a long-term variability in the subtropical anticyclone?

- If there is one, how does this variability affect TC tracks?

Chapter 2

Data

The present study is primarily based on the very large CCC400 simulation data set. Additionally, ERA-interim reanalysis data is used for validation. Finally, a best-track database for historical tropical cyclones is described, which is used as a basis for the artificial tropical cyclone tracks modeling.

2.1   CCC400 Simulation Data

The CCC400 data set was created by the climatology group at the University of Bern. It is based on the general circulation model ECHAM5.4 provided by the Max Planck Institute in Hamburg, Germany. The model is run from AD 1599 to 2005 (Bhend, 2010). There are 30 ensemble members provided that are spliced off a 30 year control run in a triangular spectral truncation at 63 wave numbers (T63 mode). This leads to a horizontal resolution of about 2° by 2°. A set of 29 variables is stored with 6-hourly resolution (3D fields on five pressure levels), and 47 variables are stored as monthly averages (3D fields on 17 levels).

The model runs were forced by several boundary conditions.The sea surface temperatures are prescribed by the interpolated reconstructions of Mann et al. (2009). Corrections for the seasonal cycle are added to this yearly reconstructions. These two corrections are calculated from interpolated HadISST1.1 sea surface temperatures of Rayner et al. (2003) and from the NINO3.4 index.

The sea ice is also taken from the HadISST1.1 data set. Unlike the sea surface temperatures, there is no seasonal cycle added to the time series. This leads to a reduced variability of sea ice, especially over the arctic region.

Land surface forcing is provided by the data of Pongratz et al. (2008) in regions with anthropogenic influence and by potential vegetation classes in the other regions (Ramankutty and Foley, 1999). However, there was a mistake in the incorporation of

5

the albedo and forest fraction. This leads to artefacts over the continents. Still, the effect on North-Atlantic circulation is expected to be small.

Volcanic aerosols are forced by ice-core reconstructions (Crowley et al., 2008) and solar irradiance is given by the reconstructions of Lean (2000).

2.2   ERA-Interim Reanalysis Data

For the validation of our model runs a reanalysis data set was used.

Reanalyses combine numerical weather prediction models with observations to obtain a best estimate of the state of the atmosphere for a given time. This has the advantage that the data is gridded with a high temporal resolution and still takes into account the observed and measured data.

Currently, one of the most reliable reanalyses is the ERA-Interim data set (Dee et al., 2011). It is provided by the European Center for Medium-Range Weather Forecasts (ECMWF). It features a 4Dvar assimilation scheme. With a horizontal resolution of T255 (roughly $1°$ by $1°$) on 60 levels it is spatially better resolved than the CCC400 data. Like the CCC400 data it has a temporal resolution of six hours. By now, the data set covers the period from 1979 to 2010, but it is being extended constantly. Detailed information to this data set can be found in Dee et al. (2011).

2.3   Historical Tropical Cyclone Tracks

As an input for the historical genesis location based TC track simulation, the HURDAT "best track data" was used. It is the official record of tropical storms and hurricanes for the Atlantic Ocean, the Gulf of Mexico and the Caribbean Sea, provided by the National Oceanic and Atmospheric Administration (NOAA) of the U.S. department of commerce (Landsea et al., 2004).

Chapter 3

Methods

In this chapter the main steps and methods used for the analyses are described. First, the evaluation of the model data is explained. Second, the choice of the index is described, which is justified both by the literature and by the variabilty of the data. In the third part an overview over the time series analysis is given and finally the simulation of tropical cyclone tracks is explained.

3.1   Evaluation of Model Data

As the CCC400 data set is not widely used yet, it was essential to first check the data quality. In a first step the variability of the mean sea level pressure (SLP) in the data set and the performance of TC tracks was investigated. After that, multiple parameters were compared to the reference dataset.

For the evaluation of the spatio-temporal variability of the NASH, monthly mean SLP values were used. Of these values different mean and standard deviations were calculated (table 3.1). Before comparing the data to ERA-interim, various 30-year periods in the CCC400 were compared. As the data has been shown to be very robust over the different periods, the most recent 30-year period (1975-2005) was chosen for the comparison to the ERA-Interim data, which spans the period 1979-2009.

Then, wind was investigated. In a first step the zonal and meridional winds were analysed on 850 hPa, 500 hPa and 250 hPa. To get the monthly wind speed, 6-hourly wind speed was calculated out of the zonal and meridional wind components in the three levels and then averaged over the month. The wind shear was also calculated on a 6-hourly basis, according to the procedure described in section 3.2, and then averaged over the months.

To compare the CCC400 to the ERA-Interim, the latter needed to be regridded onto the same grid as the CCC400. The regridding was conducted with the climate data

Table 3.1: Overview over the different mean SLP fields used for the CCC400 model evaluation. "Timemean" stands for the mean over the time period, "ensmean" for the mean over all 30 ensemble members and "timestd" stands for the standard deviation of the monthly values over the time period.

time period	function	month	Figure
1870-2005	timemean, ensmean	July	4.1a
		August	4.1b
		September	4.1c
		October	4.1d
	timestd, ensmean	July	4.1a
		August	4.1b
		September	4.1c
		October	4.1d
	timemean	July	4.2a
		August	4.2b
		September	4.2c
		October	4.2d
1975-2005	timemean	July	4.3a
		August	4.3b
		September	4.3c
		October	4.3d
		July to October (JASO)	4.4

operators (CDO) (Schulzweida and Kornblueh, 2004). A inverse-distance-weighted average of the four nearest neighbours was calculated for every new grid-point.

After regridding, the same parameters that were calculated for the CCC400 data set were now also calculated for the ERA-Interim. Finally, the differences between the CCC400 data set and the ERA-Interim were calculated for both the mean values and also the standard deviations.

3.2   Index Selection

The decadal variability of the subtropical high is most effectively looked at with an index. After enquiring literature, an own index was defined. In this section a short overview over the steps that lead to this index is given.

The most commonly mentioned index in literature for the North-Atlantic pressure systems is the North-Atlantic oscillation (NAO). Yet, for this study a very simple index was needed that is representative for the westward extension of the subtropical high. That is not the case for the NAO, as it describes the extratropical variability. For the Atlantic no specific subtropical high index was found. However, there were indices for

the North-Pacific. Lu and Dong (2001) used JJA anomalies of geopotential heights on 850 hPa and averaged them over the western part of the subtropical high. This western part they defined as the area between 110-150°W and 10-30°N. This decision was based on the high standard deviation over the subtropical area. They tried different areas and found very similar results (Lu and Dong, 2001).

As the SLP was already examined in detail, the most straightforward index for this study was to take an average SLP over a defined area and a defined time interval. Even though it is not accurate to assume the NASH to be stable over the whole season (in section 4.2.3 the variability of the NASH over the year is described), for the investigation of the decadal variability a seasonal mean is sufficient. The National Hurricane Center (NHC) of the National Oceanic and Atmospheric Administration (NOAA) defines the hurricane season in the North-Atlantic as the period between June 1st and November 30th (*National Hurricane Center*).

Here, the JASO mean was chosen, as most of the TC activity is taking place in these four months. Following the argumentation of Lu and Dong (2001), the standard deviation over time was examined (Figure 3.1). This is problematic due to the standard deviation being highest in the storm track regions. Thus, the region with the highest standard deviation is not representative for the subtropical high in the Atlantic.
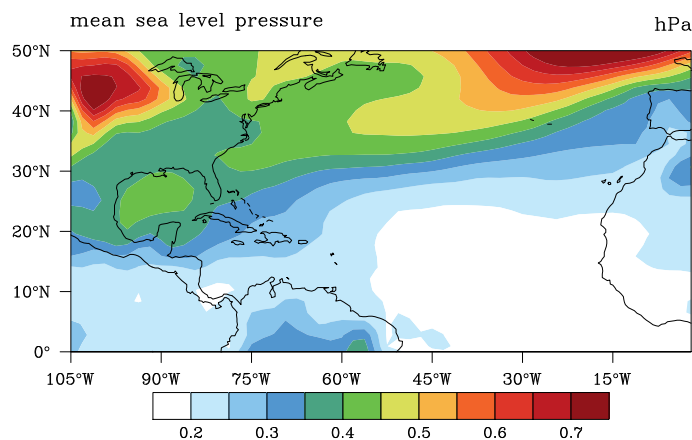

Figure 3.1: Standard deviation of CCC400 mean August ensemble mean SLP [hPa] over the years 1870-2005.

One way of eliminating the influence of the low pressure systems on the index was to choose a region where storms are not very frequent. Thus, four different area means were calculated (Table 3.2 and Figure 3.3). These four different area means behave very similarly. The correlations between the ensemble means time series are all above 0.74 (Table 3.3).

The composite difference (Figure 3.4) shows that the index is sensitive in the western part of the subtropical high, even though there are higher values in the north-eastern
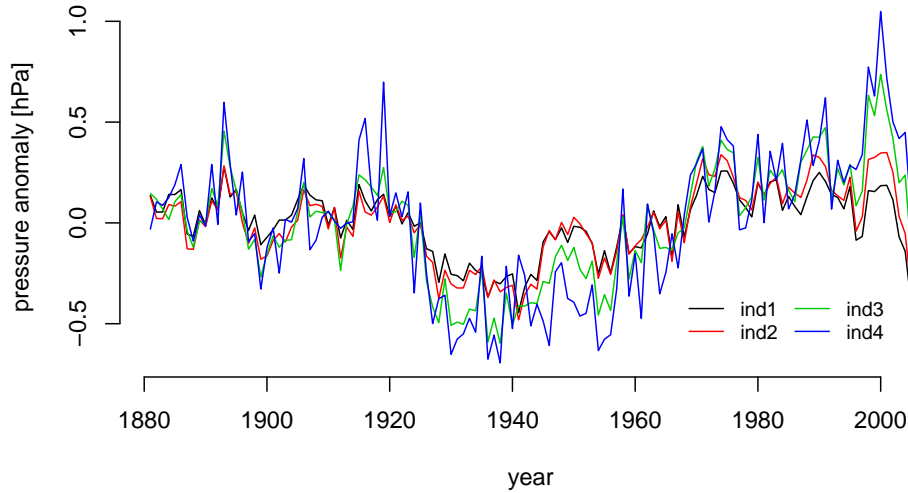
Figure 3.2: Overview over different mean SLP indices.

Table 3.2: Overview over different mean SLP boxes used for the calculation of different indices.

name	long max [°W]	long min [°W]	lat max [°N]	lat min [°N]
mean 1	60	20	30	10
mean 2	60	40	30	10
mean 3	70	50	40	20
mean 4	70	60	40	30
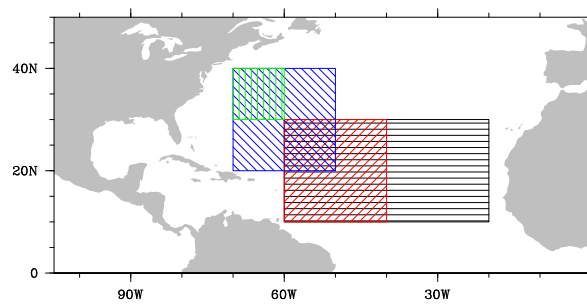
Figure 3.3: Different regions used for the calculation of the CCC400 JASO SLP mean 1 to mean 4 (black, red, blue, green).

part. This is probably due to a stronger pressure gradient in the subtropical high in this region which leads to higher absolute difference values. Surprisingly, the mean 1 has a much better pattern than mean 3, for example. This led to mean 1 being used for

Table 3.3: Correlations between different SLP mean indices.

	mean 1	mean 2	mean 3	mean 4
mean 1	1.00	0.96	0.87	0.74
mean 2		1.00	0.93	0.80
mean 3			1.00	0.94
mean 4				1.00

further analyses.
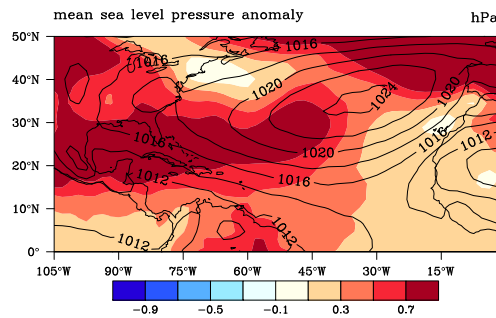
Figure 3.4: Difference between the SLP composites [hPa] of one ensemble member of all years with an index higher than 1.5 standard deviations (positive composite) and all years with an index lower than 1.5 (negative composite). The contours show the positive composite.

Another way of minimizing the influence of low pressure systems in the Atlantic on the index is to calculate maxima instead of means. When only looking at the maximum, a low pressure system should not influence the index. However, a comparison between the maximum index and the mean index showed that for the JASO mean the difference is small and the long term variability is very similar in both time series.

Even though there might be more sophisticated indices, the mean JASO SLP of the area between 60° to 20° W and 10° to 30° N was chosen. It seemed to be good enough to reproduce the long term variability of the western extension of the NASH, because the composites show a strong sign in this region, it is very robust to small scale weather systems and it is straightforward and easy to interpret.

3.3 Tropical Cyclone Tracks Simulation

It was necessary to simulate artificial tropical cyclone tracks, as in the North-Atlantic there are not a lot of TCs visible in the simulation data set. Studies have shown that there is a strong underestimation of TC intensities and number in gridded model data and the grid-size is essential (Camargo et al., 2004; Strachan et al., 2013; Walsh et al., 2010). A 2° times 2° resolution is not enough.

A very simple beta-and-advection model (BAM) was used. This method has been

introduced by Marks (1992) and has been used in various studies (Emanuel et al., 2006a; Emanuel et al., 2006b, 2008; Wu and Wang, 2004). The BAM is a very simple trajectory model that assumes that a TC is only steered by two parameters. The first one is the large scale advection ($\vec{v}_{slf}$), also referred to as steering flow or steering level flow, and the second one is the β-effect ($\vec{v}_\beta$) (equation 3.1).

$$\vec{v} = \vec{v}_{slf} + \vec{v}_\beta \tag{3.1}$$

The steering flow is defined as the weighted mean of the winds in different levels. Like in Colbert and Soden (2012), in this study only the winds in three different levels, namely at 850 hPa ($\vec{v}_{850hPa}$), at 500 hPa ($\vec{v}_{500hPa}$) and at 250 hPa ($\vec{v}_{250hPa}$) were considered, but the weights were adapted (equation 3.2).

$$\vec{v}_{slf} = \frac{3 \cdot \vec{v}_{850hPa} + 4 \cdot \vec{v}_{500hPa} + 2 \cdot \vec{v}_{250hPa}}{9} \tag{3.2}$$

The wind shear is defined as the difference between the upper level wind speed (at 250 hPa) and the lower level wind speed. The lower level wind speed is the weighted mean of the winds at the levels 850 hPa and 500 hPa. The corresponding weights are $\frac{3}{7}$ and $\frac{4}{7}$. If the wind shear between the upper and the lower levels is more than 8 m/s, the TC is assumed to only be steered by the lower levels and the 250 hPa level is neglected. Thus, the equation for the steering flow changes to equation 3.3.

$$\vec{v}_{slf} = \frac{3 \cdot v_{850hPa} + 4 \cdot v_{500hPa}}{7} \tag{3.3}$$

The β-effect is an pseudo force that acts on the TC due to the difference in Coriolis force on the northern and southern part of the TC and due to the vorticity of the TC itself. The Coriolis parameter is a function of the latitude (equation 3.4, with ω= angular velocity of the Earth [1/s] and ϕ = latitude [°]).

$$f_c = 2 \cdot \omega \cdot sin(\phi) \tag{3.4}$$

This equation shows that the Coriolis parameter f is zero at the equator and maximal at the poles. As the absolute vorticity η of an air parcel is constant, this means that if an air parcel that is moving polewards and f is getting larger, the relative vorticity ζ is getting smaller (equation 3.5). As the TC has a negative vorticity, air is moved polewards east of it and equatorwards west of it, which leads in the northern hemisphere to a negative relative vorticity advection in the north-east of the TC and a positive vorticity advection in the south-west of the TC, which then leads to a north-west drift of the TC (Figure 3.5). This effect is strongest close to the equator and is reduced towards

the poles.

$$\eta = \zeta + f = const. \tag{3.5}$$

The β-effect is calculated component-wise (equation 3.6, Marks (1992)) with u_β = u-component of the β-effect [m/s], v_β = v-component of the β-effect [m/s], ϕ = latitude of TC [°] and r = radius of TC = 300000 m.

$$u_\beta = 2 \cdot (-0.64) \cdot \beta(\phi) \cdot r^2$$
$$v_\beta = 2 \cdot 0.46 \cdot \beta(\phi) \cdot r^2 \tag{3.6}$$

β as a function of the latitude ($\beta(\phi)$) is calculated with equation 3.7. The Earth's rotation (ω) is assumed to be $7.292 \cdot 10^{-5} s^{-1}$ and the mean radius of the Earth R is 6371000 m.

$$\beta(\phi) = 2 \cdot \omega \cdot cos(\phi)/R \tag{3.7}$$

These parameters were all calculated of the two grid-points that lie closest to the position of the TC. Then the new position (λ_1, ϕ_1) was determined by integrating the velocity of the TC over six hours and adding this path to the initial position. This procedure was repeated over 40 timesteps. After these 10 days lysis of the TC was assumed, which makes the results comparable to Colbert and Soden (2012).
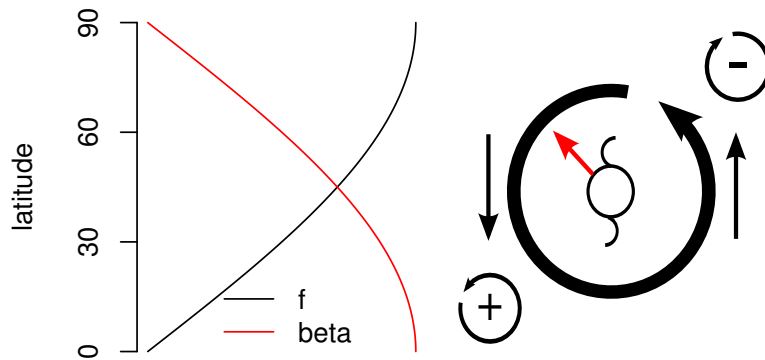
Figure 3.5: Schematic of the β-effect. Left: Coriolis-parameter f and β as a function of the latitude φ. Right: The TC is steered towards north-west due to a positive vorticity advection to the south-west of the TC and a negative vorticity advection to the north-east of the TC.

The year with the highest and lowest index was chosen. For these two years every day a TC was started at every 5° in the MDR: In the western half of the main development region (MDRW) (between 65°-45°W and 10°-30°N) and in the eastern half of the main development region (MDRE) (40°-20°W and 10°-30°N).

Additionally a simulation was started for every genesis point and date in the HURDAT dataset in the corresponding year and date in every ensemble member of the CCC400 simulation data set. Of these results then 1930-1960 and 1970-2000 were separated as periods with a very weak and a very strong subtropical high.

Chapter 4

Results

4.1 Evaluation of Model Data

In the following section the model data is evaluated by investigating different climate parameters. These include SLP, wind at different levels, the TC steering level flow and wind shear. For each parameter the variability over time was investigated. Then, the results were compared to the ERA-Interim reanalysis data.

4.1.1 Mean Sea Level Pressure

The monthly mean SLP field provides a good first impression of the circulation patterns in the North-Atlantic. It is investigated for the months of the main TC season (JASO) (Figure 4.1).

In July a very strong high pressure system is located over the North-Atlantic. Over the continents, in this case over the Sahara, low pressure systems are visible. This is the expected situation due to the the continental heat-island effect. The standard deviation is lower than $0.5\,$hPa for most of the area south of $20°\,$N and gets larger towards north-west (Figure 4.1a). In August the NASH has already weakened and the low pressure systems are also less pronounced than in July (Figure 4.1b). This weakening is also visible from August to September (Figure 4.1c) and from September to October (Figure 4.1d).

The low over North America disappears in September and in October there is a quasi-zonal border between the high (north of $20°\,$N) and the low. The standard deviation gets larger towards autumn but the patterns stay similar. In none of the months the standard deviation over the ensemble members is higher than $0.5\,$hPa.

The variability of the monthly mean SLP field over the years is smallest in July (Figure 4.2a). The mean $1020\,$hPa isobars of the different years lie close to each other.
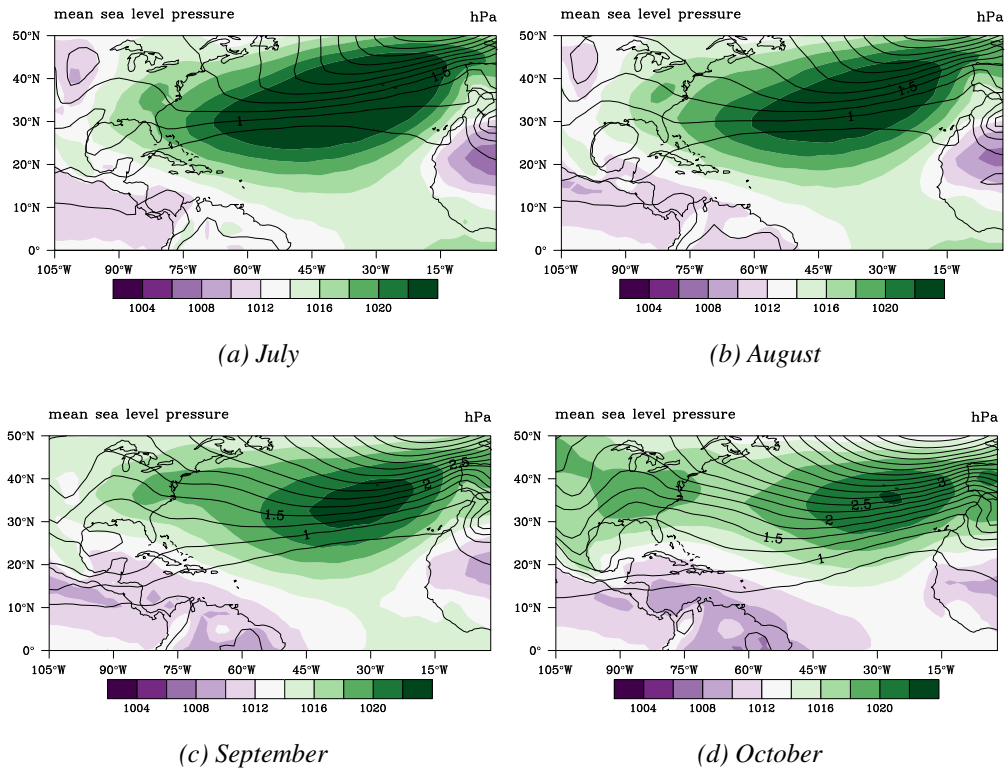
Figure 4.1: Ensemble mean July to October SLP [hPa] in CCC400 for the years 1870-2005. The black lines show the mean standard deviation [hPa] over time in steps of 0.25.
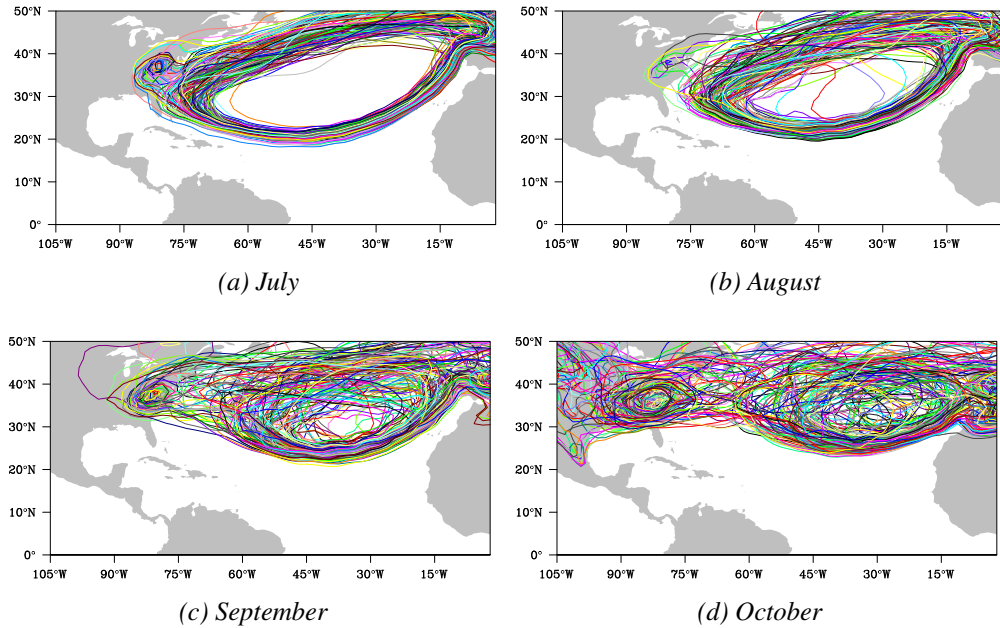

Figure 4.2: July to October yearly mean 1020 hPa contour lines for ensemble member 10 in CCC400. Every colour stands for one year between 1870 and 2005.

In the southern part the spread between the contours is only approximately 5 ° in latitude. The spread of the contours along the northern edge of the NASH is almost twice as big. The western edge of the NASH varies between almost 90 ° W and 65 ° W, but most of the lines are concentrated between 80 ° W and 70 ° W. In some years there is a separate secondary high pressure system over north-eastern North America.

In August the spread between the years is larger (Figure 4.2b). The patterns are very similar to the ones in July and in every year there is still a very pronounced high pressure system over the North-Atlantic visible. The high pressure system over North America is not that pronounced any more.

In September the differences between the years are larger than in July or August (Figure 4.2c). Remarkably, there is still a spread of less than 10° for the southern boarder of the NASH but the northern boarder is spread between 30° to 60° N. Like in July there is again a high pressure system over the North America in some of the years.

In October variability is largest (Figure 4.2d). Even though there are one or two high pressure systems visible in many years, there are also years without any well defined high pressure system over the North-Atlantic.

The isobars of the long-term monthly means of the different ensemble members (Figure 4.3) lie much closer together than the different yearly isobars. Thus, the variability between the different years is higher than the variability between the multi-

(a) July

(b) August

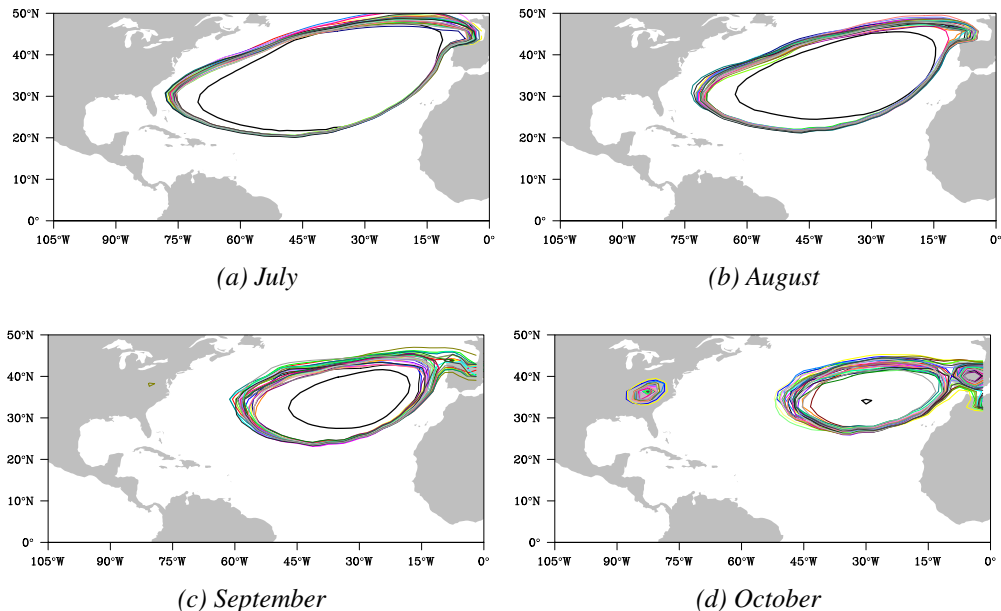*(c) September*

(d) October

Figure 4.3: July to October mean monthly mean 1020 hPa contour lines for every CCC400 ensemble member (1975-2005) in different colours and ERA-Interim (1979-2009) in bold black line.

annual mean of the different ensemble members.

Compared to the ERA-Interim data, there is a consistent overestimation of the NASH (Figure 4.4). This is the case in all months from July to October but the differences get larger towards autumn. While in summer the largest pressure differences are less than 2.5 hPa, in October they are around 3 hPa. The location of the pressure differences varies, too. While in July the highest values lie in the western North-Atlantic and over North America, the discrepancy between the two data sets in October is in the region of the NASH. The mean over the four months shows the largest errors in the same region (Figure 4.4).
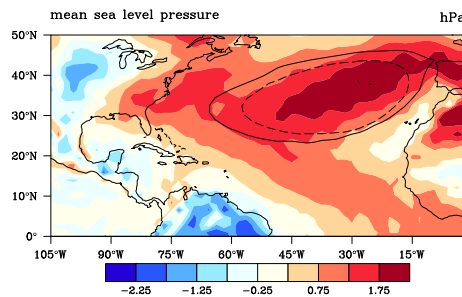
Figure 4.4: Difference between CCC400 ensemble mean and ERA-Interim JASO mean SLP fields [hPa]. The black lines show the 1020 hPa isolines for the JASO mean of the CCC400 data set for the years 1975-2006 (solid) and the ERA-Interim data set for the years 1979-2010 (dashed).

4.1.2   Merdional and Zonal Wind

Generally the wind systems in the data are what we expect. There are westerlies in the mid-latitudes and easterlies in the tropical regions. The meridional wind shows negative values in the eastern part of the North-Atlantic and positive values in the western part at 850 hPa. The opposite is true at 250 hPa. The maximum monthly mean zonal wind speed at 850 hPa level is around 10 m/s and are highest in July (>12 m/s). 500 hPa winds are slightly stronger but they do not exceed 18 m/s either. In the 250 hPa level the maxima reach more than 20 m/s in the monthly mean. The differences between the months from July to October is small, thus only August is shown (the other months are attached in the Appendix).

Compared to the ERA-Interim data, the lower level winds still are similar. The differences in most of the area are less than 2 m/s. Because the meridional winds are not very strong, their differences to the ERA-Interim are also below 2 m/s. However, the high-level zonal winds show errors of up to 20 m/s (Figure 4.5).

These errors are located very close to the equator. While there are no wester-
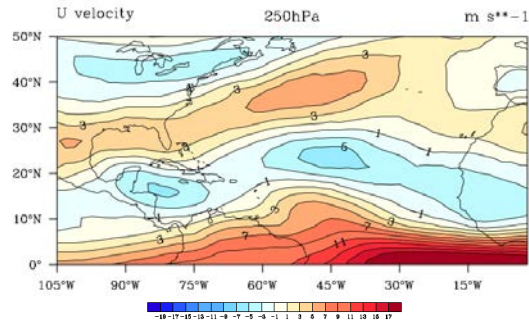
Figure 4.5: Difference between CCC400 ensemble mean and ERA-Interim 30-year mean August 250 hPa zonal wind [m/s].
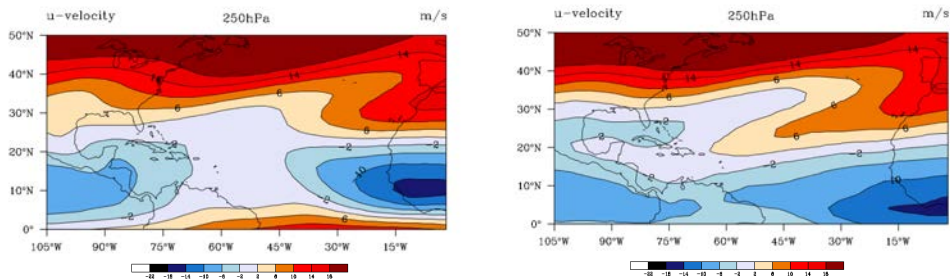

Figure 4.6: CCC400 ensemble mean (left) and ERA-Interim (right) 30-year mean August 250 hPa zonal wind [m/s].

lies around the equator in the ERA-Interim, there is a small band of westerlies in the CCC400 (Figure 4.6). The absolute values are not that different, but the pattern is shifted. Additionally, in the ERA-Interim positive zonal winds reach further to the south, especially between 60 ° W and 45 ° W.

The effect of this shift on the steering level flow and the wind shear (defined in section 3.3) are shown in the following section.

4.1.3 Steering Level Flow and Wind Shear

Relevant for the steering of the tropical cyclones is a weighted mean of the winds in different levels (steering level flow, defined in section 3.3). The figures in this section show all the parameters for August only, but from July to October there are similar patterns (see Appendix).

The zonal component of the steering level flow has values between -10 m/s and 14 m/s (Figure 4.7a, top). The separation line between positive and negative values is almost zonal and lies between 30 ° and 35 ° N. The highest positive values can be found in the very north, whereas the lowest negative values are between 10 ° and 20 ° N.

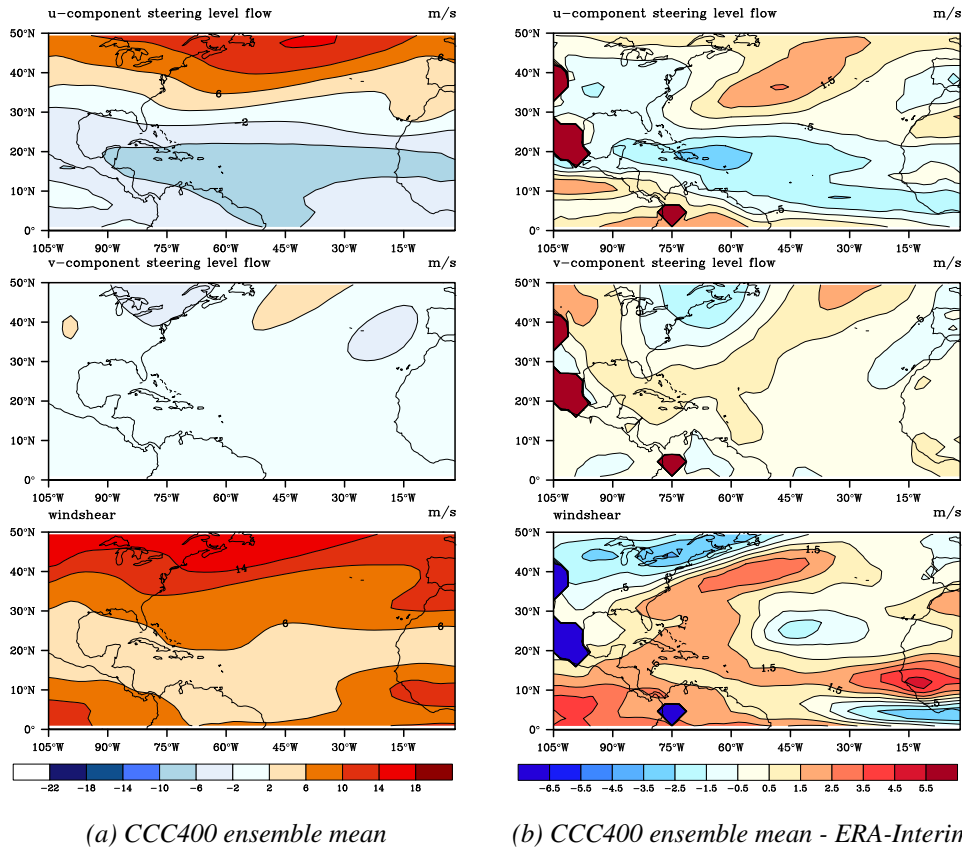(a) CCC400 ensemble mean   (b) CCC400 ensemble mean - ERA-Interim

Figure 4.7: 30-year mean August zonal and meridional component of the steering level flow and wind shear [m/s]. (a) CCC400 ensemble mean and (b) difference between CCC400 ensemble mean and ERA-Interim.

Further to the south the effect of the westerlies at the 250 hPa level weakens the easterly flow at the steering level.

The meridional wind speed is over large parts of the North-Atlantic between -2 m/s and 2 m/s. In the mid-latitudes, the effect of the Rossby waves is visible but the values do not exceed 6 m/s in either direction. There are two southerly flows visible, one over central North America and one over the central North-Atlantic. In between there two northerly flows. One lies over eastern Canada and the other one in front of the western coast of the Iberian Peninsula and North Africa.

The wind shear between the upper and the lower levels (as defined in section 3.1) ranges from 2 m/s to 18 m/s (Figure 4.7a, bottom). The highest values lie in the very north, the lowest values around 20 °N.

As we can see in Figure 4.7b (top), the large differences in the 250 hPa zonal winds (subsection 4.1.2) is not that important for the steering flow and therefore it is negligible for the beta-advection model. The absolute values of the differences do not exceed 3.5 m/s. However, there is an overestimation of the zonal wind over the Atlantic

in latitudes of 30 °N and more. In the lower latitudes there is an underestimation.

Differences in meridional wind speed do not exceed 2.5 m/s (Figure 4.7b, middle). There is a slight overestimation in the central North-Atlantic and a slight underestimation over eastern Canada and western Europe and west of the North African west coast.

The mean monthly wind shear shows differences to the ERA-Interim over most of the North-Atlantic (Figure 4.7b), which is due to the different circulation patterns in the upper level (Figure 4.1.2). The area where a typical TC track lies shows an overestimation of wind shear of 1.5 m/s to 4.5 m/s. Compared to the critical wind shear value of 8 m/s used for the calculation of the steering level flow, this overestimation is not negligible. Where the NASH lies, there is an underestimation of up to 2.5 m/s. Noticeable are also the strong gradients over the eastern Canadian east coast and in the south west. Implications of that bias will be discussed later.

4.2   Variability of the Subtropical High Index

In this section the variability of the NASH is examined. This is done by means of the index defined in section 3.2, i.e. SLP averaged over the region 60° W to 20° W, 10° N to 30° N. First the variability between ensemble members is shown, then the seasonal variability and finally the question if there is an decadal variability is answered.

4.2.1   Variability between Ensemble Members

The differences between the long-term means of the different ensemble members are all below 0.2 hPa and all ensemble members show very similar distributions (Figure 4.8).

In an individual year the ensemble spread between the maximum and the minimum is up to 3 hPa (Figure 4.9). The spread of the 25th to 75th percentile is around 0.5 hPa. Despite the large spread of the ensemble members, there is a common variability visible. This long-term variability is described in section 4.2.2.

4.2.2   Decadal Variability

One of the aims of this study was to investigate the long-term variability of the NASH in the data. As discussed before, there is in all ensemble members a common long term variability visible (Figure 4.9). This decadal variability is further investigated in this section using the ensemble mean.

The 10-year running mean of the ensemble mean suggests a variability in the period of roughly 20-30 years (Figure 4.10). This is also confirmed by the wavelet-analysis (Figure 4.11, lower panel), even though this variability is not over the whole time period statistically significant at a level of 95%.

Even more pronounced than this is a variability in the period of 60-90 years, with a total maximum in 72 years. It is statistically significant over the whole time period between 1600 and 2005 at a confidence level of 95%. A variability over the centuries is also suggested, but to prove this an even longer time period is needed.

Not only is there a statistically significant decadal variability in the time series, but also a linear decreasing trend. It is slightly decreasing and significant at a level of 95% (Figure 4.11, upper panel).
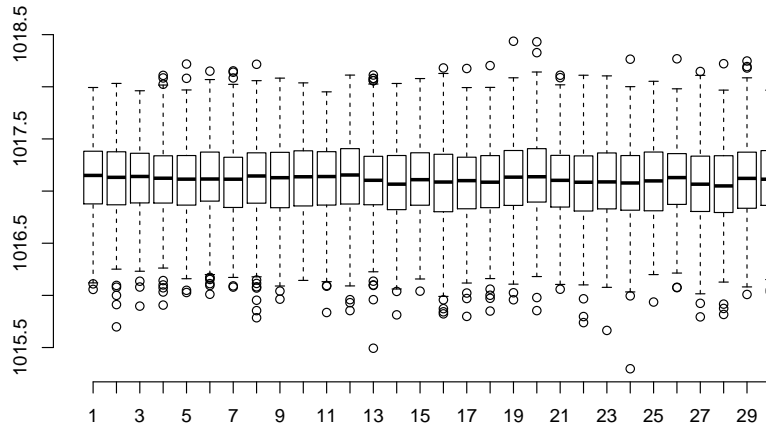
Figure 4.8: Boxplot of all CCC400 ensemble members. The x-axis shows the ensemble members. The y-axis shows the mean JASO SLP [hPa] (60-20W, 10-30N) of the years 1880-2010.
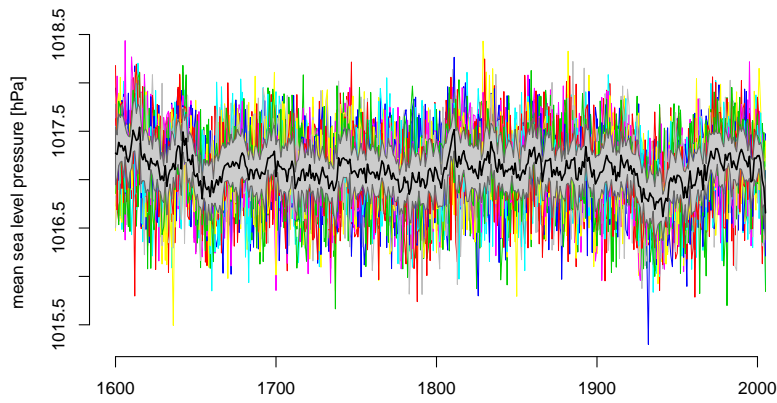

Figure 4.9: JASO mean SLP (60-20W, 10-30N) for all CCC400 ensemble members (colours), ensemble mean (black), 75 and 25 percentiles (grey) of the years 1600-2005.
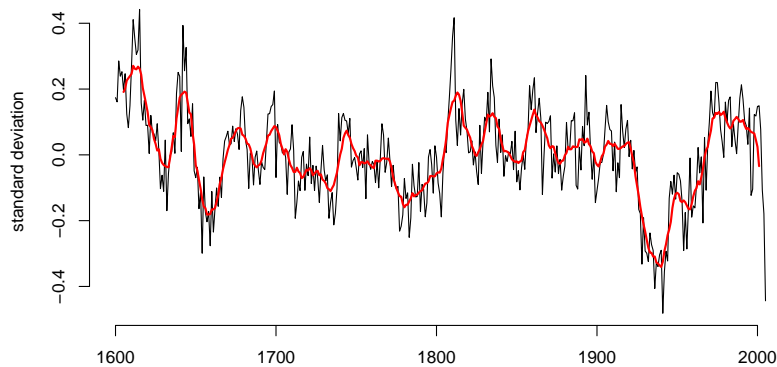

Figure 4.10: Mean JASO SLP anomaly (60-20W, 10-30N) of the years 1600 to 2005 with reference to the mean over the whole time period and normalized with the standard deviation . In red the corresponding 10-year running mean.
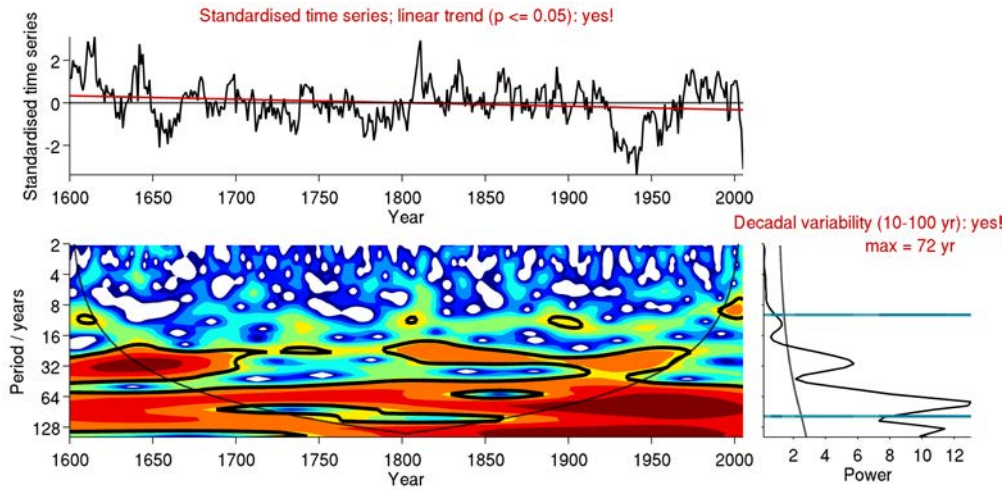
Figure 4.11: Output of the wavelet analysis. Top: Standardised time series of the JASO mean SLP anomaly of the ensemble mean (60-20W, 10-30N) (black) with corresponding trend (red). Bottom: Continuous wavelet power spectrum as a function of time. The thick black contour designates the 5% significance level against red noise and the cone of influence is separated by the thin black line. On the right the power spectrum is depicted as a function of the period. (Figure provided by Christoph Welker)

Atlantic Multidecadal Oscillation

The decadal variability of the NASH has a maximum at the period of 72 years. One Atlantic mode that has a similar periodicity is the AMO (Figure 4.12). The AMO is connected with anomalous high sea surface temperatures in the North-Atlantic. There is a negative linear correlation of 0.71 between the 10 years running mean of the AMO and the mean JASO SLP anomaly (60-20W, 10-30N). For the yearly time series the correlation is lower, with a correlation coefficient of -0.50.
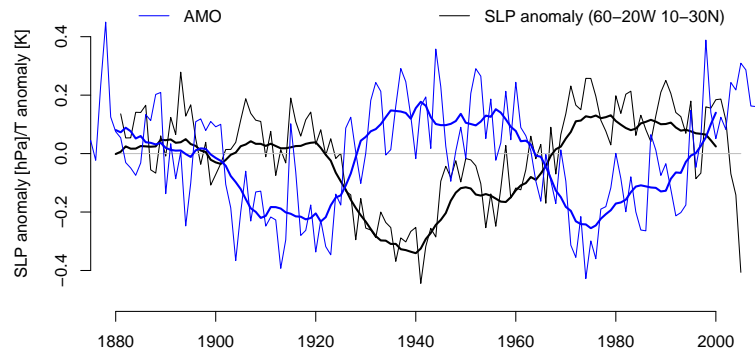
Figure 4.12: AMO (blue), mean JASO SLP anomaly of the ensemble mean (60-20W, 10-30N) (black) of the years 1880 to 2005 and the corresponding 10 years running means (bold).

4.2.3 Seasonal Variability

There is a strong seasonal cycle in the NASH (Figure 4.13). The 1880-2005 mean NASH is strongest in June and July and weakens fast to the absolute minimum in October and November. The mean anomaly of the July mean with reference to the JASO mean is 1.5 hPa, in August it is 0.7 hPa, in September -0.4 hPa and in October -1.8 hPa with a mean spread of 3.1 hPa. Additional to the largest deviation from the JASO mean, October has also the largest year-to-year variability of these four months.

In most of the years the succession from high SLP in summer towards lower SLP in autumn is observed. Only in a few cases the order is changed. However, an anomalously high July SLP does not mean high October SLP, too (Figures 4.14 and 4.15). While the correlation between August and October is almost zero, the correlation between the other months is roughly around 0.2. Interestingly, October shows a correlation with July that is still 0.2.
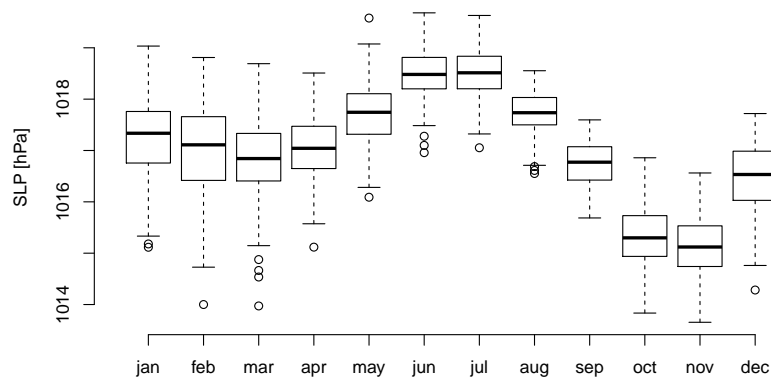
Figure 4.13: Boxplot of the CCC400 mean SLP (60-20W, 10-30N) of the years 1880-2005 for every month (ensemble mean).
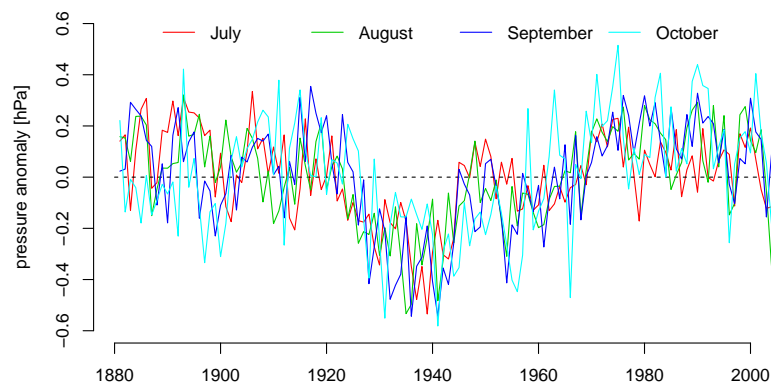
Figure 4.14: Monthly SLP anomalies (60-20W, 10-30N) of the CCC400 ensemble mean with reference to the 1880-2005 monthly mean.
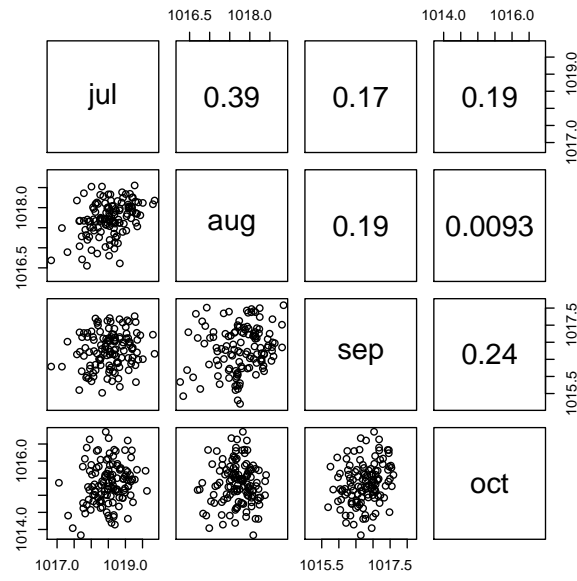
Figure 4.15: Pearson correlation coefficients between CCC400 ensemble mean July to October monthly mean SLP (60-20W, 10-30N) from 1880 to 2005 and the corresponding scatter plots.

4.3 Tropical Cyclones

In the following section tropical cyclones are investigated. First the performance of TCs in the CCC400 model data is shortly discussed, then the results of the TC track simulation are presented.

4.3.1 Tropical Cyclones in the Model Data

Low pressure systems that form in the tropics and have paths that resemble TCs are visible in the model data. However, due to the rather coarse resolution of the model, TC-like cyclones in the data do not reach the intensity of TCs. The number of TCs per season is also underestimated in the model data. Therefore a synthetic TC track simulation was carried out using a beta-and-advection model on the CCC400 data set.

4.3.2 Simulated TCs

In this section the results of the TC-track simulation with help of the beta-and-advection model are presented. First the experiment with seeded starting points is shown and second the experiment with historical starting points is shown.

Seeded Starting Points

As mentioned before, there are two main parameters that influence the TC tracks. On one hand the genesis location is important, on the other hand the large-scale steering flow. To be able to understand the influence of the steering flow, the seeded experiment was divided into four different parts. There was a simulation with starting points in the eastern half of the main development region and a simulation with the starting points in the western half. Both simulations were carried out for two different years, one having a very positive NASH anomaly and one having a very negative NASH anomaly.

The density of TC tracks in the simulation with the western starting points is in both cases highest over the western part of the Caribbean. Most of the TCs are steered towards the Caribbean Islands and Florida (Figure 4.16a, left).

In the case where the NASH is stronger, there is a weaker TC density around the genesis location and over most of the Caribbean (4.17a, right). In return, the density over Central America and over large parts of the US East Coast is higher.

The simulation with starting points in the east shows a different TC track distribution. Compared to the west experiment the TC density is shifted more towards the east. Less tracks hit the US coast or the Caribbean Islands. The general pattern is more zonal than in the west experiment (Figure 4.16b, left).

The year with a positive NASH anomaly has a higher density of TC tracks in south-west of the NASH. More TCs reach the Caribbean Islands and fewer TCs pass the region north of the development region between roughly 45°W and 20°W (Figure 4.16b, right and Figure 4.17b).

Despite the differences in the density of TC tracks, the median track is very similar for the positive NASH anomaly year and the negative NASH anomaly year (Figure 4.18a). For the case with starting point in the west, there is no difference visible. In the case of an eastern starting point, the median track of the positive anomalous year is shifted towards the west, compared to the one in the negative anomalous year.

Historical Starting Points

In this section the results of the simulation of TC tracks with historical genesis locations are presented. There are two experiments executed. The first one is performed for all ensemble members in the period between 1970 and 1999, which was a period of a fairly strong NASH in the CCC400 data and the second one was carried out for all ensemble members and the period from 1930 to 1960, which was a period of weak NASH.

In the period where the NASH was more intense, the TC tracks are broader distributed. A maximum intensity is reached over the northern Gulf of Mexico, Florida and west of it as far as 70°W. But the intensity gradient is flat and the tracks are distributed over the whole western part of the North-Atlantic.

In the 30 years with a negative NASH anomaly, the distribution is more pronounced. The maximum is situated in the south-western part of the Gulf of Mexico. Many tracks are also visible over the Caribbean Islands.

Compared to the period with the negative NASH anomaly, in the period with a positive anomaly there are some differences. First, there are more tracks in the region between 60° to 20° W and 10° to 20° N. Second, there is a positive anomaly over the North-Atlantic and the U.S. East Coast north of roughly 20° N. And finally there is a strong negative anomaly over the Caribbean Islands, the Gulf of Mexico and Central America.

Looking at the median track in both cases, we see that the median starting points much more in the east than in the seeded experiments. They are situated roughly 65°W in the case of the positive NASH anomaly and 70°W in the negative one. The shift between the positive and negative periods tracks is between 5° and 15°.

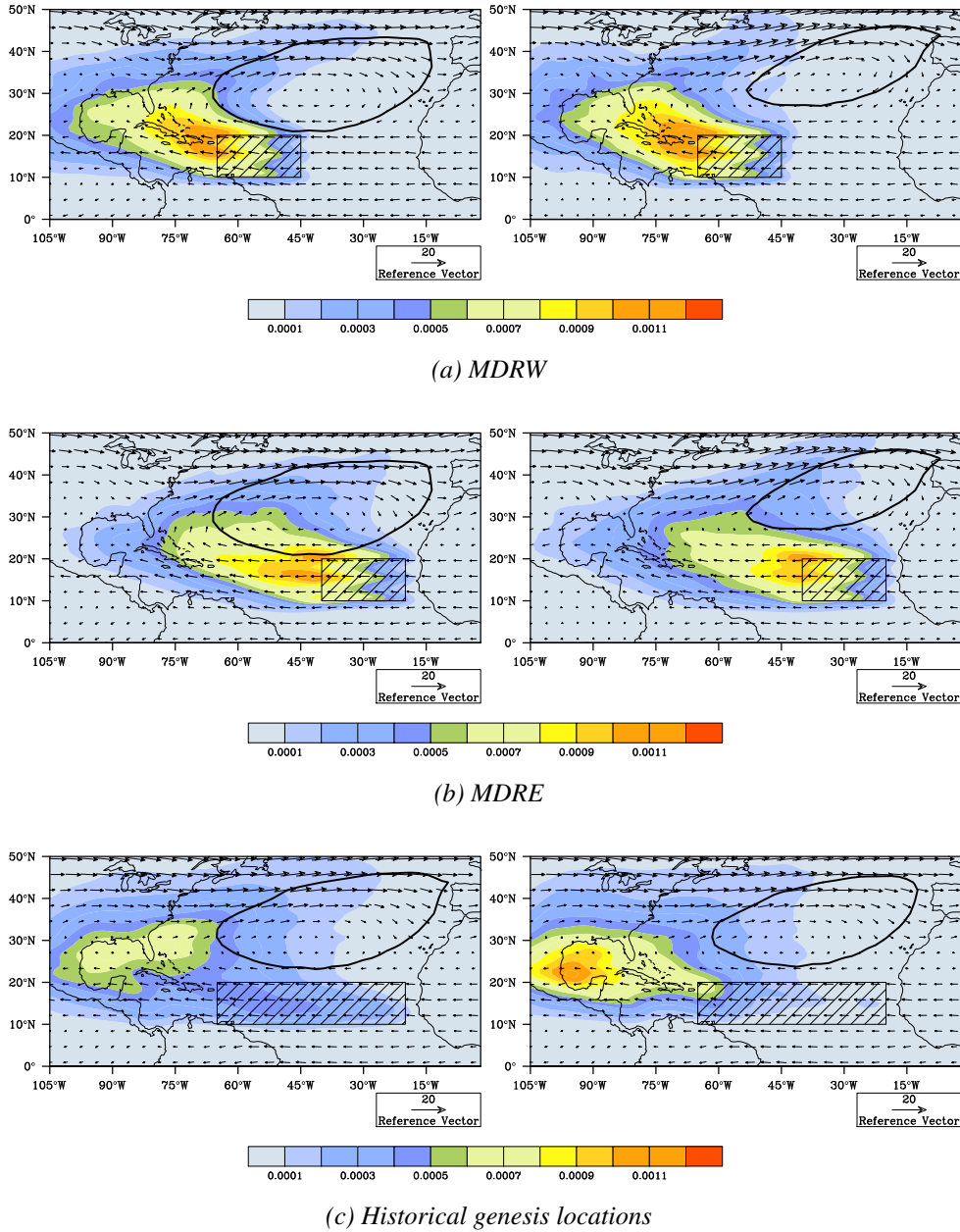*(a) MDRW*

(b) MDRE

(c) Historical genesis locations

Figure 4.16: Density distribution of the simulated TC tracks with (a) western, (b) eastern and (c) historical genesis locations. The region where the starting points were seeded is shaded. In black the JASO mean 1020 hPa SLP contour line is shown. The arrows show the JASO mean steering level flow [ms^{-1}].
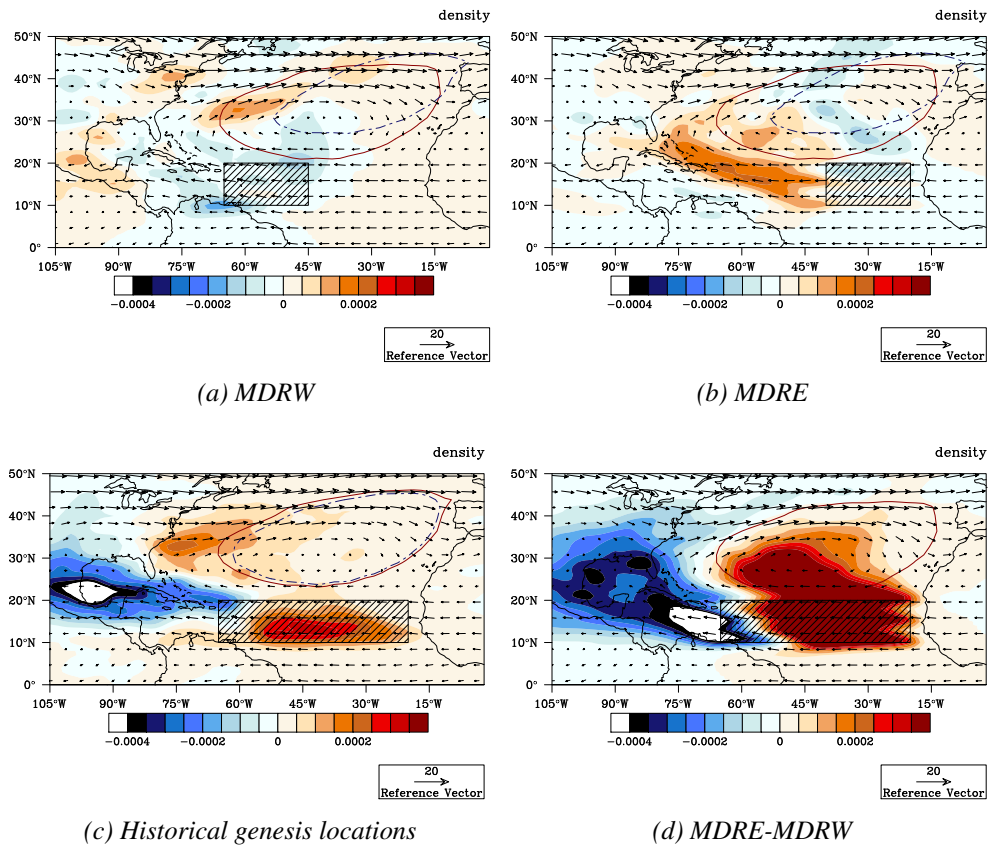
(a) MDRW

(b) MDRE

(c) Historical genesis locations

(d) MDRE-MDRW

Figure 4.17: Difference in simulated TC track density between the positive anomalous and the negative anomalous NASH time period with (a) western seeding region, (b) eastern seeding region and (c) historical genesis locations. In (d) the difference in simulated track density between the eastern and western experiment in a year with positive NASH anomaly is shown. The contours show the JASO mean 1020 hPa SLP for the positive (red) and negative (blue, dashed) period and the arrows show the JASO mean steering level flow $[ms^{-1}]$ in the positive period

(a) MDRW and MDRE

(b) Historical genesis locations
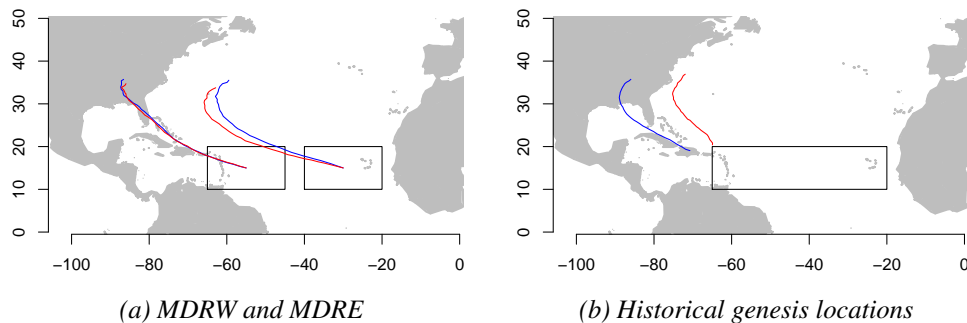
Figure 4.18: Median of the simulated TC tracks of the (a) seeded and (b) historical experiments. Blue (red) shows the tracks for the simulation runs with a negative (positive) NASH anomaly.

Chapter 5

Discussion

5.1 Evaluation of the Model Data

Generally the CCC400 dataset has proven to be a good tool to investigate the North-Atlantic circulation patterns. There are, however, some biases in the dataset that need to be taken into account. The most prominent feature is a systematic overestimation of the NASH. This overestimation is present for the whole TC season (JASO) and amounts to 2 hPa in the JASO mean. As this study concentrates on the influence of the NASH on TC tracks, the main focus is on relative changes of the SLP field and the TC tracks. Thus, the overestimation of the NASH does not impact the results much. However, it has to be taken into account that absolute values are biased.

As a consequence the wind is also biased. While the winds at 850 hPa and at 500 hPa are very similar to the ERA-Interim reanalysis data, the strength of zonal winds in the upper levels is overestimated. This is in accordance with the bias in the pressure fields. As the high pressure system is more pronounced, this leads to a stronger anticyclonic flow over the North-Atlantic, resulting in stronger easterlies in the tropics and stronger westerlies in the mid-latitudes. This effect is amplified in the upper levels, as the pressure gradient is stronger in the upper levels. However, there is an additional feature which is not explained by the the NASH. In the CCC400 dataset there are westerlies at the 250 hPa level in the very low latitudes (<5°N), which are not present in the ERA-Interim data. This leads to very strong anomalies in the zonal winds, which could have substantial impact on the simulated tropical cyclone tracks. The reasons for this bias should be investigated thoroughly before using the dataset in tropical regions. However, for the seeded experiment it is not so much of a problem because the starting points lie all north of 10°N.

The strong NASH and the resulting strong anticyclonic flow in the upper level lead to substantially increased wind shear values around the NASH (1.5 m/s - 2.5 m/s).

This causes the simulated TC to pass the critical wind shear threshold of 8 m/s earlier. When the wind shear is higher than the threshold, the upper level winds are not taken into account in the beta-and-advection model. This has the side-effect that anomalous high upper level winds do not influence the simulated TC tracks.

5.2   Variability of the Subtropical High Index

Despite the overestimation of the NASH, its monthly variability is similar to the one in the ERA-interim. Generally the NASH is quite variable within one year. The highest linear correlation between two adjoining months is between July and August with roughly 0.4. Even with a lag of 3 months, the autocorrelation is still 0.2 (October and July). Only the correlation between October and August is very low, which is astonishing, because the remaining months all show substantially higher autocorrelations of 0.2. In some cases the strength of the NASH does not decrease systematically from July to October. This is consistent with the results of Davis et al. (1997), who propose the extent and intensity of the NASH to be very variable and to show half-month periods. As supposed by Sahsamanoglou (1990) October shows the weakest NASH. In addition to the large month to month variability and the strong variability between the different ensemble members, the JASO ensemble mean shows long-term variability.

The power spectrum of the JASO ensemble mean shows three statistically significant maxima. The strongest oscillation has a period of approximately 70 years. Gray et al. (1997) and Goldenberg et al. (2001) have shown that there is a multidecadal oscillation in the North-Atlantic SST, which has a similar period. The positive mode of this oscillation, also named AMO, is associated with a stronger thermohaline circulation in the North-Atlantic. This leads to higher SSTs in the northern North-Atlantic and lower SSTs in the tropical North-Atlantic (Goldenberg et al., 2001). In this study a negative correlation of -0.51 was found between the AMO and the strength of the NASH in the ensemble mean on a yearly basis (see Figure 4.12). This in accordance with the results of Klotzbach and Gray (2008) who found a correlation of -0.5 between the SLP over the North-Atlantic (70-10W, 0-50N) and the SSTs in the northern North-Atlantic (50-10W, 50-60N) significant at the 99% level. The 10- year running mean of our SLP index in the ensemble mean and the 10-year running mean of the AMO correlate with an even higher coefficient of -0.7.

5.3   Tropical Cyclones

The CCC400 data set contains TC similar low pressure systems. However, the intensity and the number of TCs are substantially underestimated. Most of the features that resemble TCs do not even reach TC intensities in the CCC400 data. Especially

in the Atlantic the discrepancy between the observed and the subjectively identified TC number in CCC400 is large. This is most probably due to the model resolution. Camargo et al. (2004) have proven that the model resolution has a strong influence on the number and intensity of TCs present in the data. The deficiencies of coarse resolution models are high in the North-Atlantic. This is not only due to weaknesses in the simulated storm dynamics, but also is there an underestimation of the TC genesis potential (Bengtsson et al., 2006). The resolution needed for an accurate representation of the number of TCs per season is roughly 130 km. For a correct representation of the distribution of TCs in a basin the resolution should even be 100 km or less (Strachan et al., 2013).

The simulated TC tracks with the seeded experiment show the influence of the large scale advection (and therefore the NASH) on one hand and the influence of the genesis location of the TCs on the other hand. The strength of the NASH, defined as the JASO mean SLP between 60-20°W and 10-30°N (see section 3.2), has different influences on the simulated TCs that started in the MDRE than on the TCs started in the MDRW.

The west experiment shows that a positive NASH index leads to fewer TCs around the MDRW. As the track density is calculated of the location of the TCs every 6 hours, this pattern alludes to a faster TC movement. This hypothesis is supported by the two mean wind fields (i.e. Figure 4.16a) showing slightly increased wind speeds in the year with a positive NASH index. The strongest positive TC track anomaly is between 70-45°W and 30-35°N (Figure 4.16b), which means that more of the storms are steered back towards Europe. It is not possible to say whether the risk of land falling is affected by the NASH index by viewing this picture. The risk for a land falling TC could be higher for Central America, Mexico and the northern US-West-coast north of roughly 35°N. However, results have to be taken carefully because it is possible that the anomalies in density are mainly due to different propagation speed of the simulated TCs.

The east experiment shows a different behaviour. There is like in the west experiment a negative track density anomaly for the year with a positive NASH index in the development region, in this case the MDRE. But there is a distinct positive density anomaly west of the MDRE. Additionally there are less tracks north of the MDRE. This is most probably due to the south-west shift of the NASH that steers the TC further to the west. Therefore the number of TCs making landfall in the Caribbean Islands is larger. There are less tracks that reach the higher latitudes (>35°N). It is questionable that this effect would be that pronounced in real track data. The simulated tracks only last 10 days, which means that if they are steered more towards the west, there is less time left for the TC to recurve.

The influence of the NASH is much weaker than the influence of the seeding re-

gion. There is mainly an east-west gradient in the difference between the two density distributions. TCs that developed in the MDRE stay more east than TCs started in the MDRW. This very simple result could be artificially enhanced in this experiment, because the TCs only last for 10 days. A more realistic duration of the storm might allow more tracks of the MDRE to reach the Gulf of Mexico or the US-Coast.

Summarising that, the seeded experiments are in accordance with the results of Colbert and Soden (2012). Even the JASO mean the NASH has an influence on TC tracks in this experiment. Colbert and Soden (2012) also stated that the variability of the genesis location plays an important role for the TC track variability, which was confirmed in our experiment.

The distribution of the starting points of the seeded experiment a strong simplification. The observed distribution of TC genesis locations shows indeed a maximum in the MDR, but there are also many tracks that start further west, namely in the Gulf of Mexico (Murakami and Wang, 2010) (Figure 5.1). Therefore the results can not directly be transferred to the real TC distributions. A more realistic view on the influence of the NASH on the TC tracks could provide the experiment with historical TC genesis locations. There were two beta-and-advection model runs for 30 years with a strong NASH (1970-1999) and a weak NASH (1930-1960). As an input the genesis locations of the HURDAT best-track dataset of the corresponding years were taken.
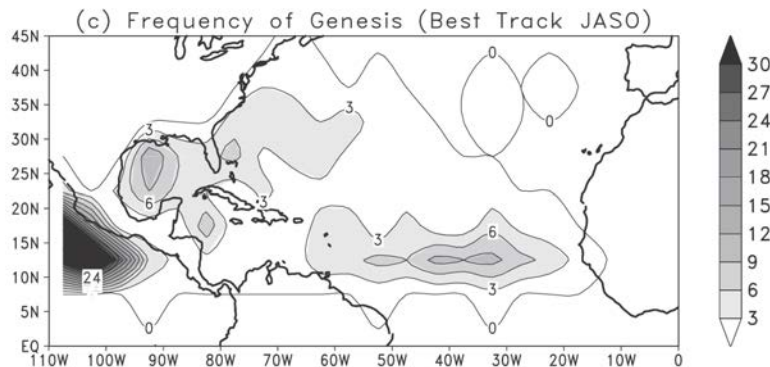
Figure 5.1: JASO mean of frequency of TC genesis based on the best-track data between 1851 and 2005 (Murakami and Wang, 2010, adapted)

The simulated differences in this case look more like the seeded west experiment than the seeded east experiment. This yields to the assumption, that the chosen starting points in the seeded experiments are too far east, which is consistent with the observation of TC genesis locations depicted in Figure 5.1. The differences between the positive NASH years and the negative NASH years, however, do not have much in common with the west experiments. The pattern look similar to the difference between the east and west experiment.

A first hint for a shift in genesis locations between the period with a strong NASH

and a weak NASH (1970-2000 and 1930-1960) is given by the shift of the median track (Figure 4.18b). The movement of the TC after the genesis is very similar in both cases. The influence of the genesis location predominates and the influence of the NASH strength is very small. Comparing the observed shift in genesis locations in Holland (2007) (Figure 5.2), with the simulated change in track density, the assumption that the genesis location is the main factor for the different track densities is confirmed. The two anomaly fields of these densities look very similar. There were more TCs developing in the south-east and the north-west during the second half of the twentieth century than in the first half, and less TCs developing in the south-west.
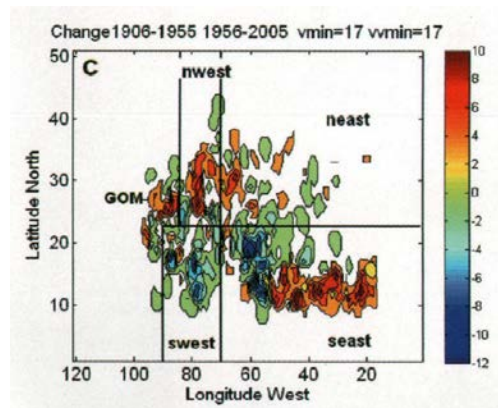
Figure 5.2: Change in TC genesis density from 1906-1955 to 1956-2005 (Holland, 2007, adapted)

The simulated track distribution difference between the late (1970-99) and the early (1930-59) twentieth century is very close to the trend over the whole twentieth century in the observed HURDAT tracks (Figure 5.3). Only the observed positive anomaly over Central America is not represented in the simulation. This means on one hand that the simulation of the TC tracks started at the historical TC genesis locations in all ensemble members leads to a realistic distribution of TC tracks. The advantage of the simulation is, that for each genesis location there are 30 different possible tracks, which could be of use in risk assessments. On the other hand the question is whether this shift is due to natural long-term variability and shows an oscillating behaviour or whether it is a linear trend, like Vecchi and Knutson (2008) postulated.

There are three different hypotheses for the reasons for the change in genesis location. The first one is not actually a shift, but a reduction in TC formation. Landsea et al. (1994) have found a reduction of the TC tracks in the Caribbean from the period 1944-1967 to the period 1986-1991. This study also shows the reduction in the Caribbean that fits their analyses. However, they postulated a reduction in overall TC activity in the North-Atlantic due to unfavourable conditions for TC genesis, namely increased shearing winds and a decreased percentage of strong easterly waves. This can not be the case for the time windows in this study, as there is almost the same
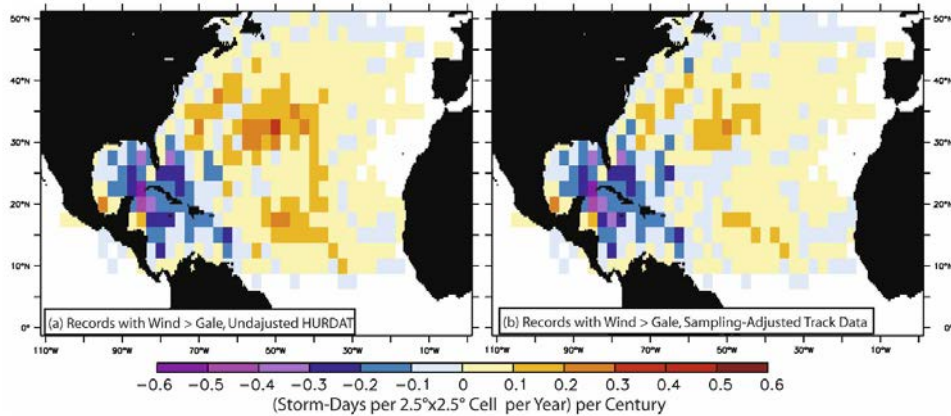
Figure 5.3: Linear trend in TC density over 1878–2006 for the unadjusted HURDAT database (left) and for the sampling density change adjusted database (Vecchi and Knutson, 2008)

number of tropical cyclones in the HURDAT data set (193 to 196 tracks).

Another reason for a shift in TC genesis location could be a bias in the early observational data. TCs could have been detected later in their development in the early twentieth century, as weak cyclonic systems were difficult to detect in the eastern North-Atlantic (Holland, 2007). This has little effect on the total number, but leads to an eastward shifted genesis location. However, Vecchi and Knutson (2008) adjusted the HURDAT data set for the sampling density change during the twentieth century and could still observe the strong decrease in TC tracks in the Caribbean and the Gulf of Mexico, but with a less pronounced increase in the western North-pacific.

The third reason could be a change in the TC genesis potential in the North-Atlantic. Emanuel and Nolan (2004) invented a genesis potential index, that has proven to be a good measure for the TC activity in a region (Camargo et al., 2007). It takes into account low level absolute vorticity and relative humidity, wind shear and a potential intensity that is calculated by means of dissipate heating, SST, SLP and temperatures and mixing ratios at different levels. As Goldenberg et al. (2001) and references therein stated, the most important parameters for TC formation are high SST and low wind shear (Goldenberg et al., 2001). The SST in the tropical Atlantic were almost the same in the two periods. Wind shear might have played an important role.

Under the assumption that the AMO will weaken in the close future, the SLP index will rise. This could lead to a further eastward shift of the TC track distribution. Murakami and Wang (2010) predict such a shift for the future. However, to support this prediction, much more analyses would be needed.

Chapter 6

Conclusions

In this study the impact of long-term variability of the North-Atlantic subtropical high-pressure system (NASH) on tropical cyclone (TC) tracks was examined. The basis was a 400-year simulation data set that was used to generate artificial TC tracks with a beta-and-advection model. The following main results were found:

- The North-Atlantic circulation patterns are generally well represented in the CCC400 data. However, there is a systematic overestimation of the NASH, which leads to biases in the wind fields. Especially in the upper levels close to the equator the wind fields do not seem accurate.

- Despite some biases in the CCC400 data it shows good results in the simulation of TC tracks. The dataset is suitable for investigating the influence of different parameters on TC tracks.

- The NASH shows a long-term variability with a maximum in the period of 72 years. This variability is anti-correlated with the Atlantic Multidecadal Oscillation.

- The strength of the NASH does directly influence the distribution of the TC tracks. The effect is different depending on the genesis location of the TC tracks. While the simulated TCs developing in the eastern part of the main development region (MDR) tend to stay longer over the tropical ocean, the ones developing in the western part tend to recurve more in the year with a strong NASH.

- The change in simulated TC track distribution between the periods 1930-1959 and 1970-1999 is dominated by a shift in genesis location towards the east, which makes it impossible to assign any difference to a change in steering flow. To have a more complete picture, more knowledge of the interaction between the NASH and the genesis point should be gained.

Appendix
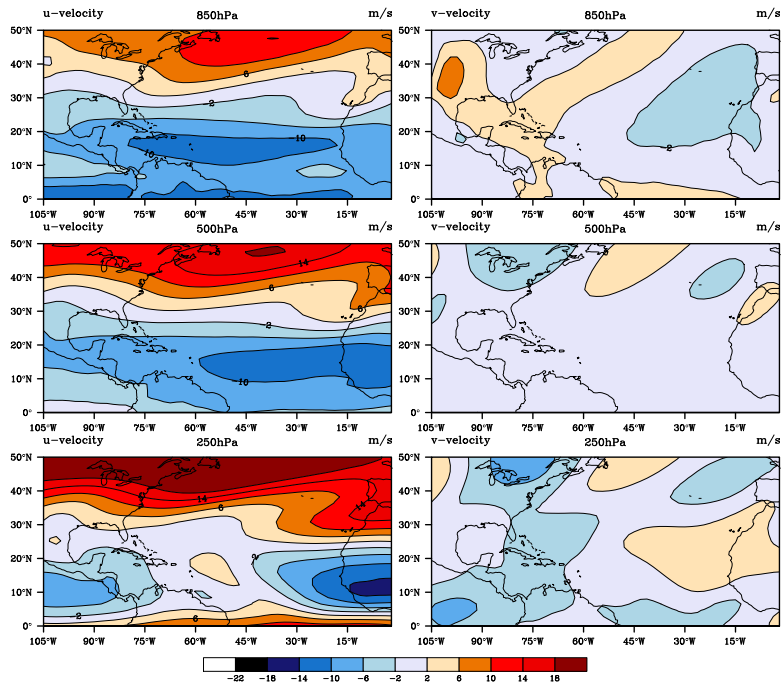
(a) CCC400 ensemble mean
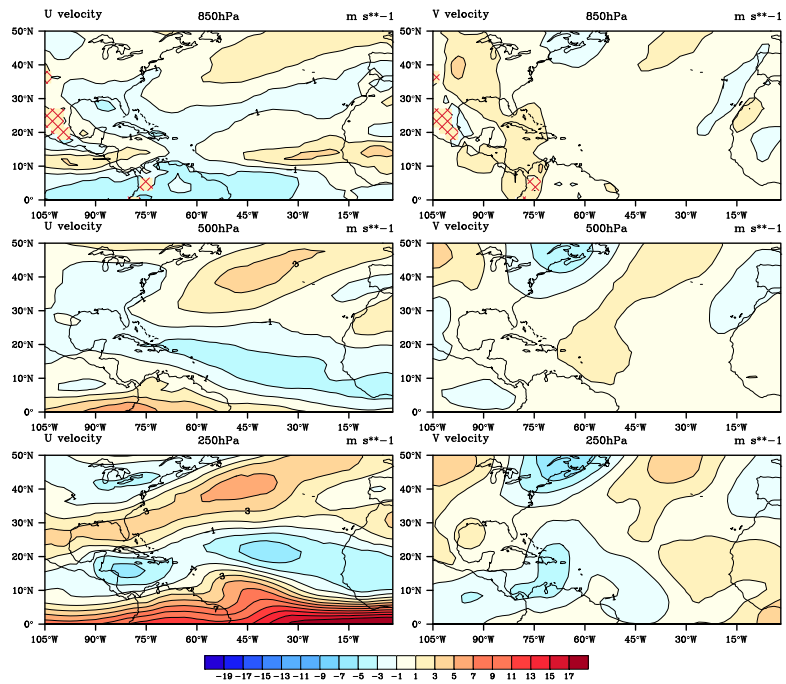
(b) CCC400 ensemble mean - ERA-Interim

Figure 6.1: 30-year mean July zonal and meridional wind at 850 hPa, 500 hPa and 250 hPa. (a) CCC400 data and (b) difference between CCC400 and ERA-Interim
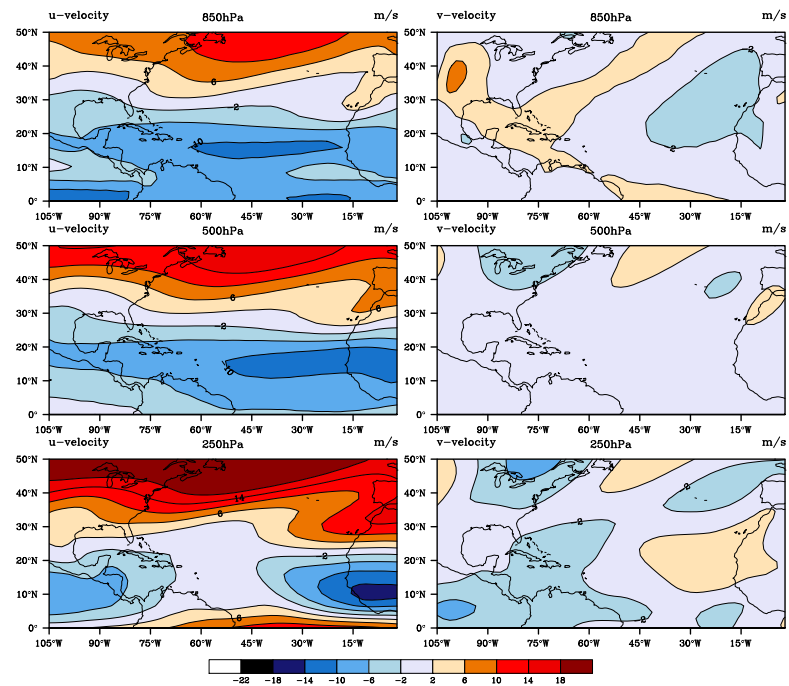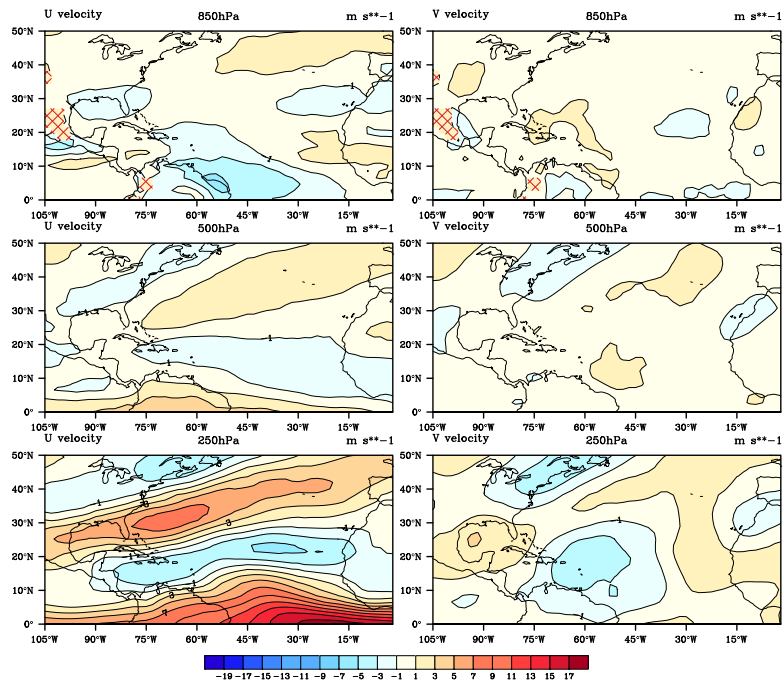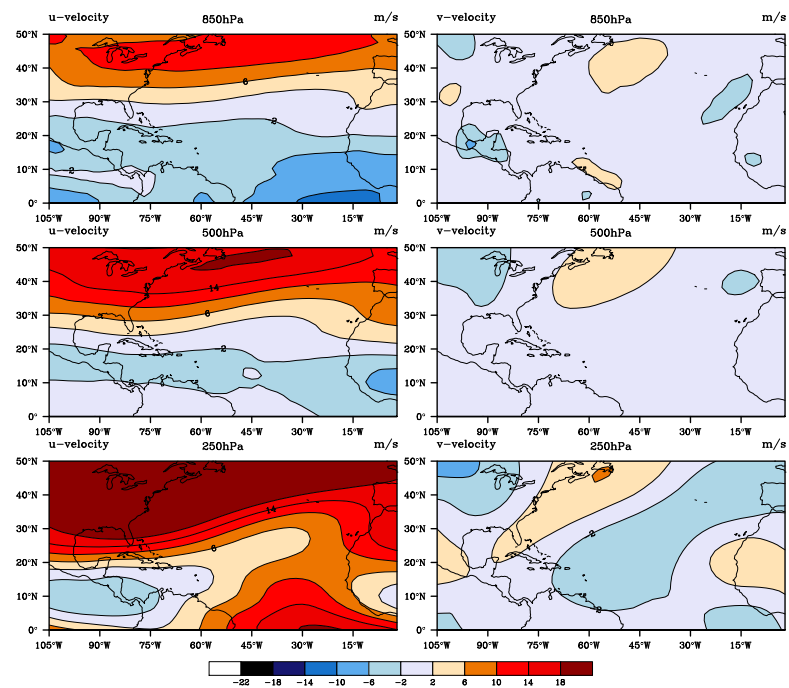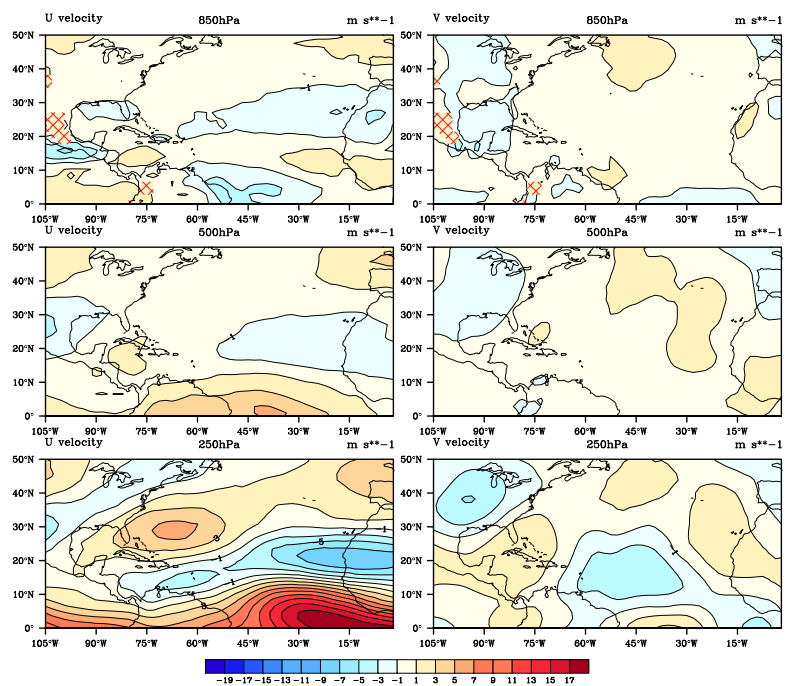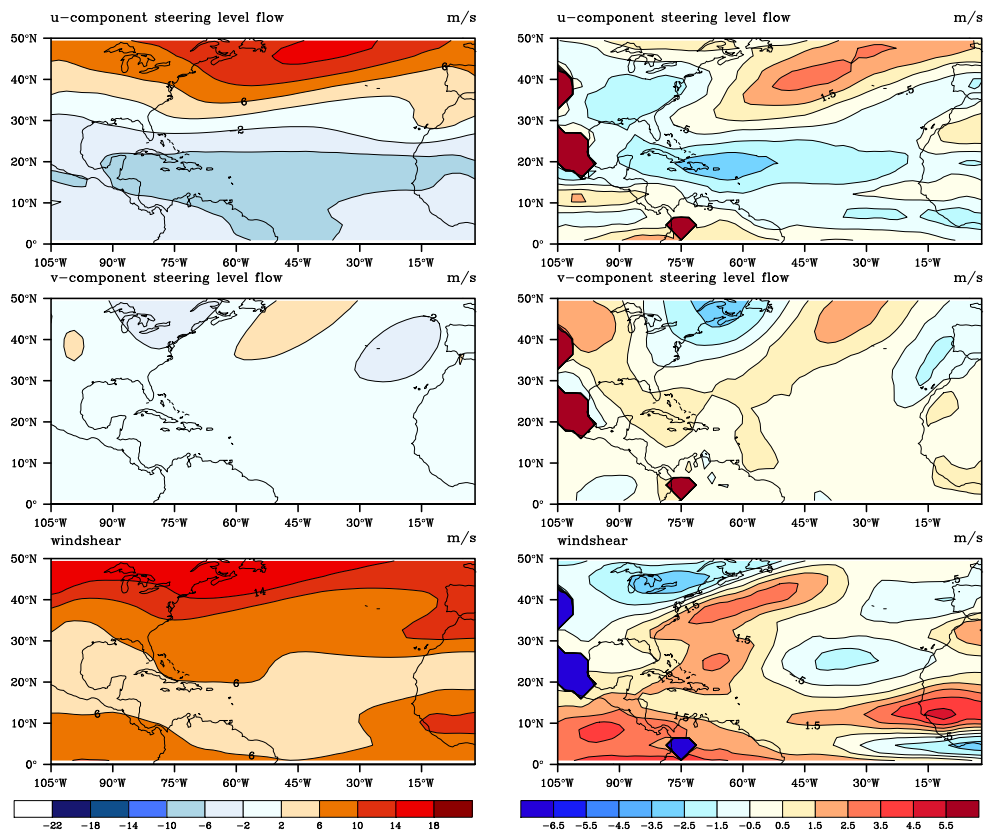
(a) CCC400 ensemble mean
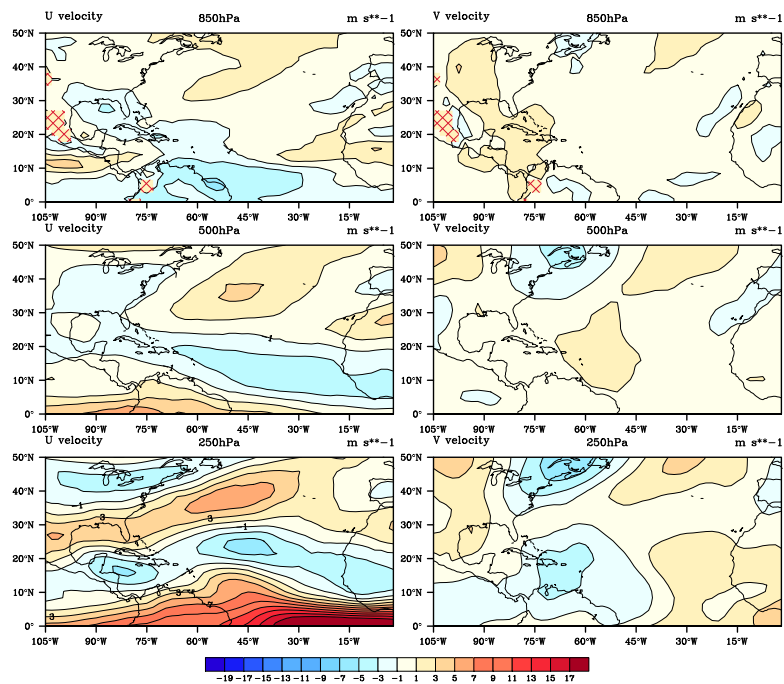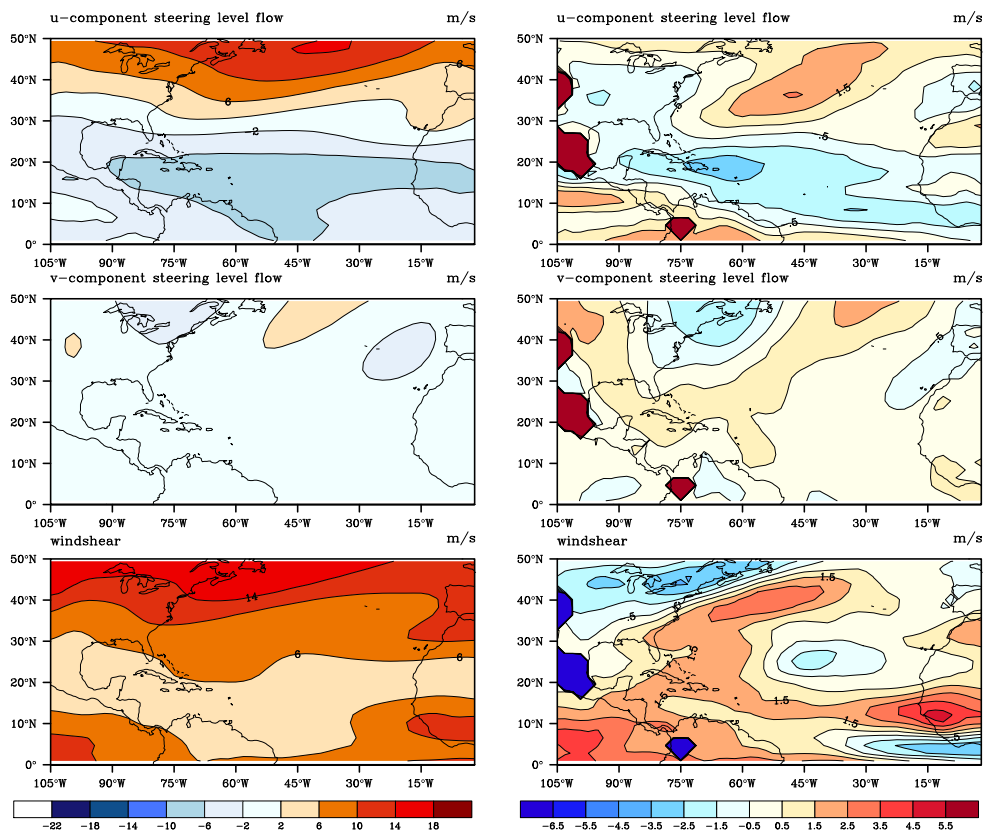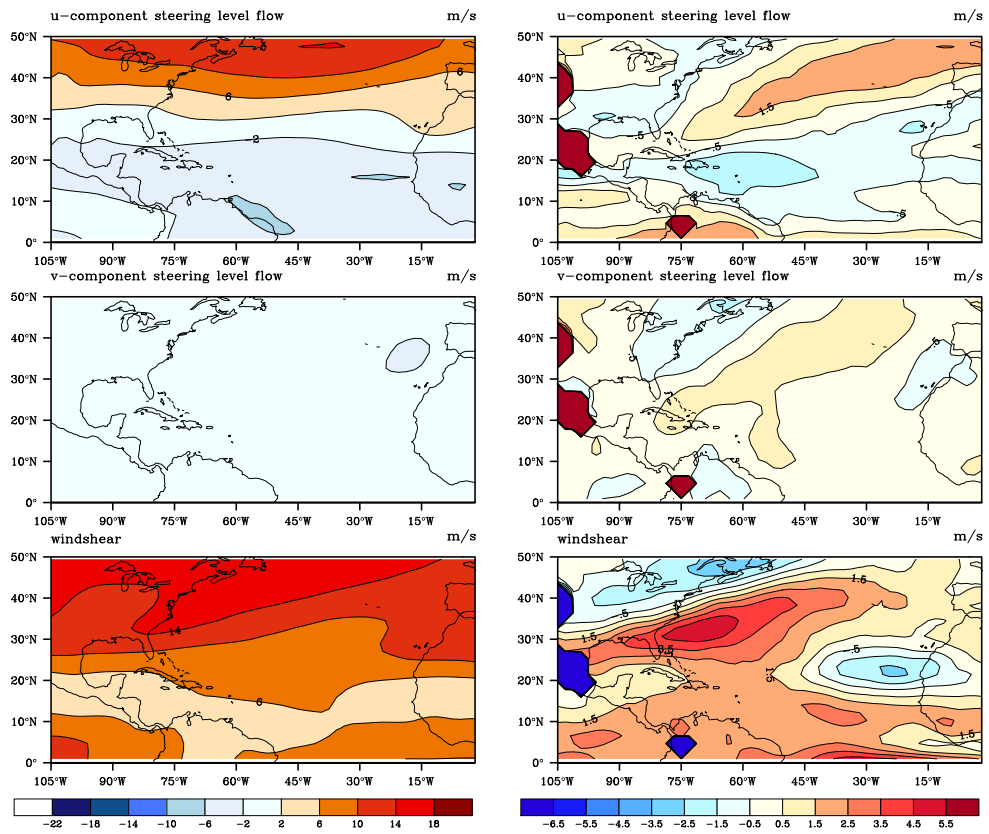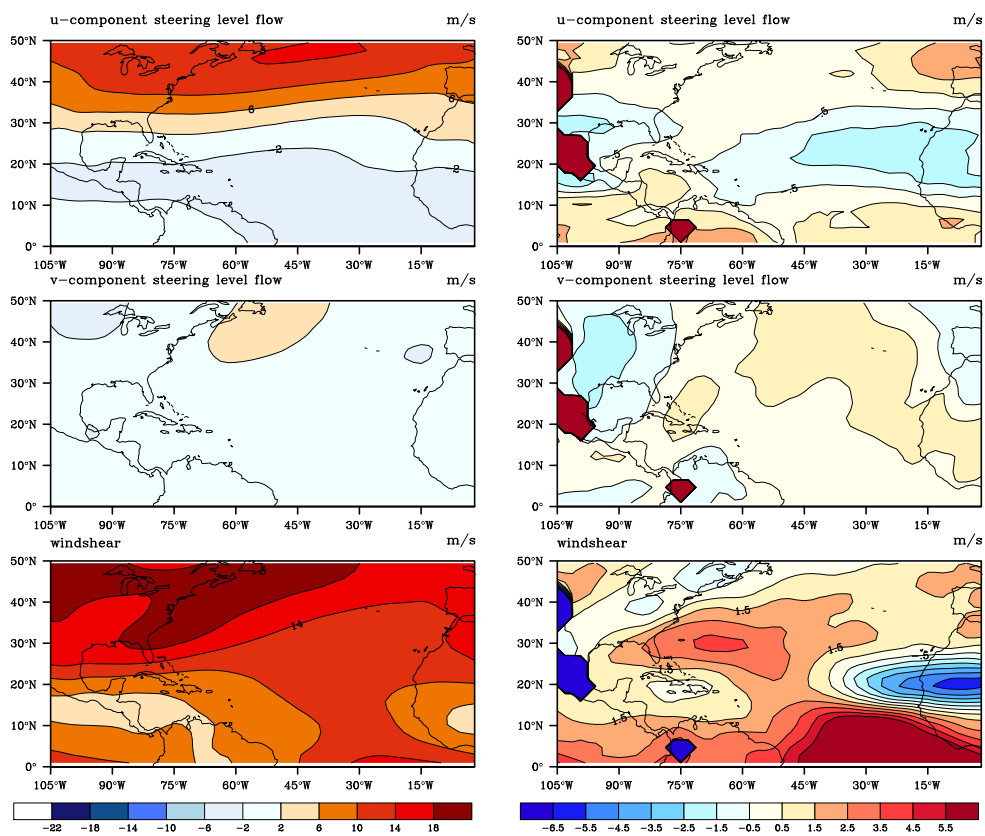

(b) CCC400 ensemble mean - ERA-Interim

Figure 6.2: 30-year mean August zonal and meridional wind at 850 hPa, 500 hPa and 250 hPa. (a) CCC400 data and (b) difference between CCC400 and ERA-Interim
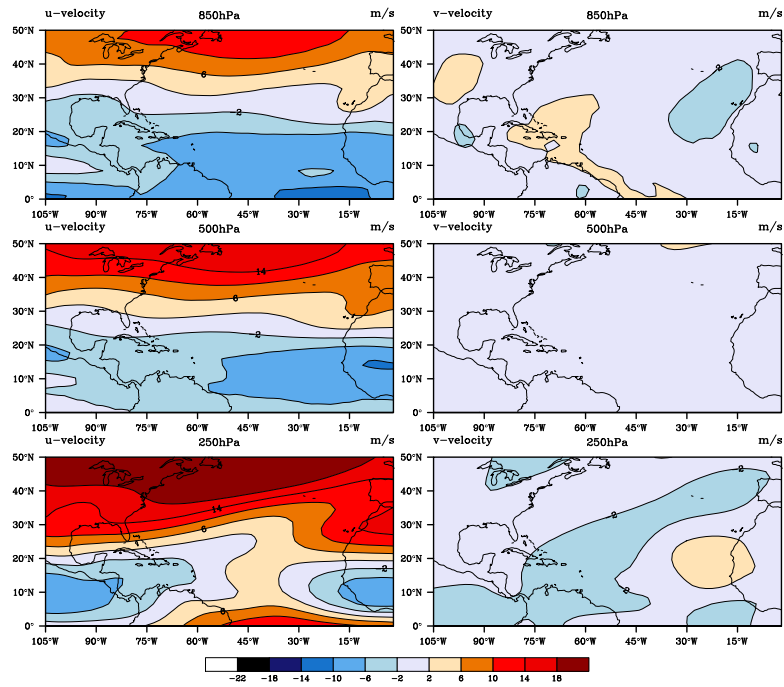
(a) CCC400 ensemble mean

(b) CCC400 ensemble mean - ERA-Interim

Figure 6.3: 30-year mean September zonal and meridional wind at 850 hPa, 500 hPa and 250 hPa. (a) CCC400 data and (b) difference between CCC400 and ERA-Interim

(a) CCC400 ensemble mean

(b) CCC400 ensemble mean - ERA-Interim

Figure 6.4: 30-year mean October zonal and meridional wind at 850 hPa, 500 hPa and 250 hPa. (a) CCC400 data and (b) difference between CCC400 and ERA-Interim

(a) CCC400 ensemble mean   *(b) CCC400 ensemble mean - ERA-Interim*

Figure 6.5: 30-year mean July meridional and zonal steering level flow and wind shear. (a) CCC400 data and (b) difference between CCC400 and ERA-Interim

(a) CCC400 ensemble mean

(b) CCC400 ensemble mean - ERA-Interim

Figure 6.6: 30-year mean August meridional and zonal steering level flow and wind shear. (a) CCC400 data and (b) difference between CCC400 and ERA-Interim

(a) CCC400 ensemble mean   *(b) CCC400 ensemble mean - ERA-Interim*

Figure 6.7: 30-year mean September meridional and zonal steering level flow and wind shear. (a) CCC400 data and (b) difference between CCC400 and ERA-Interim

(a) CCC400 ensemble mean

(b) CCC400 ensemble mean - ERA-Interim

Figure 6.8: 30-year mean October meridional and zonal steering level flow and wind shear. (a) CCC400 data and (b) difference between CCC400 and ERA-Interim

Acronyms

AMM Atlantic Multidecadal Oscillation.

AMO Atlantic Multidecadal Oscillation.

BAM beta-and-advection model.

ENSO El-Niño Southern Oscillation.

JASO July to October.

MDR main development region.

MDRE eastern half of the main development region.

MDRW western half of the main development region.

NASH North-Atlantic subtropical high-pressure system.

SLP mean sea level pressure.

SST sea surface temperature.

TC tropical cyclone.

List of Figures

List of Tables

Bibliography

AMS glossary. last modified on 25 June 2013, at 07:08. URL: http://amsglossary.allenpress.com/glossary.

Bengtsson, L., Hodges, K. I. and Roeckner, E. (2006). "Storm tracks and climate change". In: *Journal of Climate* 19.15, pp. 3518–3543.

Bhend, J. (2010). "Setup and maintenance of the CCC400 simulations with ECHAM5.4".

Camargo, S. J. et al. (2007). "Tropical cyclone genesis potential index in climate models". In: *Tellus A* 59.4, pp. 428–443. ISSN: 1600-0870.

Camargo, S. J., Barnston, A. G. and Zebiak, S. E. (2004). *Properties of Tropical Cyclones in Atmospheric General Circulation Models.* English. Tech. rep. International Research Institute for Climate Prediction. URL: http://hdl.handle.net/10022/AC:P:8806.

Colbert, A. and Soden, B. (2012). "Climatological variations in North Atlantic tropical cyclone tracks". In: *Journal of climate* 25.2, pp. 657–673.

Crowley, T. J. et al. (2008). "Volcanism and the little ice age". In: *Pages News* 16.2, pp. 22–23.

Davis, R. E. et al. (1997). "The North Atlantic subtropical anticyclone". In: *Journal of Climate* 10.4, pp. 728–744.

Dee, D. et al. (2011). "The ERA-Interim reanalysis: Configuration and performance of the data assimilation system". In: *Quarterly Journal of the Royal Meteorological Society* 137.656, pp. 553–597.

Della-Marta and Prechtl (2010). *The CatFocus Tropical Cyclone Model: Advanced Risk Analysis and Validation.* Tech. rep. PartnerRe.

Elsner, J. B. (2003). "Tracking hurricanes". In: *Bulletin of the American Meteorological Society* 84.3, pp. 353–356.

Emanuel, K et al. (2006a). "Supplement to A Statistical Deterministic Approach to Hurricane Risk Assessment". In: *Bulletin of the American Meteorological Society* 87.3, s1–s5.

Emanuel, K. et al. (2006b). "A statistical deterministic approach to hurricane risk assessment". In: *Bulletin of the American Meteorological Society* 87.3, pp. 299–314.

Emanuel, K., Sundararajan, R. and Williams, J. (2008). "Hurricanes and global warming: Results from downscaling IPCC AR4 simulations". In: *Bulletin of the American Meteorological Society* 89.3, pp. 347–367.

Emanuel, K. A. and Nolan, D. (2004). "Tropical cyclone activity and the global climate system". In: *Preprints, 26th Conf. on Hurricanes and Tropical Meteorology, Miami, FL, Amer. Meteor. Soc. A*. Vol. 10.

Fink, A. H. and Speth, P. (1998). "Tropical cyclones". In: *Naturwissenschaften* 85.10, pp. 482–493.

Goldenberg, S. B. et al. (2001). "The recent increase in Atlantic hurricane activity: Causes and implications". In: *Science* 293.5529, pp. 474–479.

Gray, W. M. (1984). "Atlantic seasonal hurricane frequency. Part I: El Niño and 30 mb quasi-biennial oscillation influences". In: *Monthly Weather Review* 112.9, pp. 1649–1668.

Gray, W. M., Sheaffer, J. D. and Landsea, C. W. (1997). "Climate trends associated with multidecadal variability of Atlantic hurricane activity". In: *Hurricanes*. Springer, pp. 15–53.

Holland, G. J. (2007). "Misuse of landfall as a proxy for Atlantic tropical cyclone activity". In: *Eos, Transactions American Geophysical Union* 88.36, pp. 349–350.

Klotzbach, P. J. and Gray, W. M. (2008). "Multidecadal variability in North Atlantic tropical cyclone activity". In: *Journal of Climate* 21.15, pp. 3929–3935.

Knutson, T. et al. (2010). "Tropical cyclones and climate change". In: *Nature Geoscience* 3.3, pp. 157–163.

Kossin, J. P. and Vimont, D. J. (2007). "A more general framework for understanding Atlantic hurricane variability and trends". In: *Bulletin of the American Meteorological Society* 88.11, pp. 1767–1781.

Kossin, J., Camargo, S. and Sitkowski, M. (2010). "Climate modulation of North Atlantic hurricane tracks". In: *Journal of Climate* 23.11, pp. 3057–3076.

Landsea, C. (2007). "Counting Atlantic tropical cyclones back to 1900". In: *Eos, Transactions American Geophysical Union* 88.18, pp. 197–202.

Landsea, C. W. et al. (1994). "Seasonal forecasting of Atlantic hurricane activity". In: *Weather* 49.8, pp. 273–284.

Landsea, C. W. et al. (2004). "The Atlantic hurricane database re-analysis project: Documentation for the 1851–1910 alterations and additions to the HURDAT database". In: *Hurricanes and Typhoons: Past, Present and Future*, pp. 177–221.

Lean, J. (2000). "Evolution of the Sun's spectral irradiance since the Maunder Minimum". In: *Geophysical Research Letters* 27.16, pp. 2425–2428.

Li, W. et al. (2012). "Intensification of Northern Hemisphere subtropical highs in a warming climate". In: *Nature Geoscience* 11, 830–834.

Lu, R. and Dong, B. (2001). "Westward extension of North Pacific subtropical high in summer." In: *Journal of the Meteorological Society of Japan. Ser. II* 79.6, pp. 1229–1241.

Mann, M. E. et al. (2009). "Atlantic hurricanes and climate over the past 1,500 years". In: *Nature* 460.7257, pp. 880–883.

Marks, D. G. (1992). *The beta and advection model for hurricane track forecasting*. Tech. rep. US Department of Commerce, National Oceanic and Atmospheric Administration, National Weather Service, National Meteorological Center.

Murakami, H. and Wang, B. (2010). "Future Change of North Atlantic Tropical Cyclone Tracks: Projection by a 20-km-Mesh Global Atmospheric Model*". In: *Journal of Climate* 23.10, pp. 2699–2721.

National Hurricane Center. last modified on June 27, 2013 at 17:30. URL: http://www.nhc.noaa.gov/.

Pongratz, J et al. (2008). "A reconstruction of global agricultural areas and land cover for the last millennium". In: *Global Biogeochemical Cycles* 22.3.

Ramankutty, N. and Foley, J. A. (1999). "Estimating historical changes in global land cover: Croplands from 1700 to 1992". In: *Global biogeochemical cycles* 13.4, pp. 997–1027.

Rayner, N. et al. (2003). "Global analyses of sea surface temperature, sea ice, and night marine air temperature since the late nineteenth century". In: *Journal of Geophysical Research: Atmospheres (1984–2012)* 108.D14.

Sahsamanoglou, H. (1990). "A contribution to the study of action centres in the North Atlantic". In: *International Journal of Climatology* 10.3, pp. 247–261.

Schulzweida, U and Kornblueh, L (2004). "Climate Data Operators". In: *Max-Planck-Institute for Meteorology, Hamburg*. URL: http://www.mpimet.mpg.de/cdo.

Strachan, J. et al. (2013). "Investigating global tropical cyclone activity with a hierarchy of AGCMs: the role of model resolution". In: *Bulletin of the American Meteorological Society* 26, pp. 133–152.

Trenberth, K. (2005). "Uncertainty in hurricanes and global warming". In: *Science(Washington)* 308.5729, pp. 1753–1754.

Vecchi, G. A. and Knutson, T. R. (2008). "On Estimates of Historical North Atlantic Tropical Cyclone Activity". In: *Journal of Climate* 21.14, pp. 3580–3600.

Walsh, K. et al. (2010). *The tropical cyclone climate model intercomparison project*. English. Springer.

Wu, L. and Wang, B. (2004). "Assessing Impacts of Global Warming on Tropical Cyclone Tracks*". In: *Journal of climate* 17.8, pp. 1686–1698.

Xie, L. et al. (2005). "Climatology and interannual variability of North Atlantic hurricane tracks". In: *Journal of climate* 18.24, pp. 5370–5381.

Acknowledgements

I would like to express my gratitude to Olivia Romppainen and Stefan Brönniman for supervising this thesis, answering all my questions, providing a lot of feedback and suggestions for my work and always taking the time even while being off university.

I also want to thank Paul Della-Marta for allocating the beta-and-advection model, bearing all my emails and sharing his expertise with me. Further I would like to thank Jörg Franke for helping me with all the data-relevant questions, Christoph Welker for conducting the wavelet analysis and Richard Wartenburger for passionately fixing my computer problems again and again.

A special thank goes to the whole fifth floor in the GIUB for cordially welcoming me into the group and spending many interesting coffee and lunch breaks together. And last but not least, I would like to thank my family and my friends for their support, the proof reading, the cakes and chocolates and for all the encouraging words.

Declaration

under Art. 28 Para. 2 RSL 05

Last, first name: Lenggenhager, Sina

Matriculation number: 07-056-005

Programme: M.Sc. in Climate Sciences

Bachelor ☐   Master ☒   Dissertation ☐

Thesis title: Tropical Cyclone Tracks and the Subtropical High Pressure
                     System in the North-Atlantic in a 400-year Climate Simulation

Thesis supervisor: Prof. Dr. Olivia Romppainen-Martius

I hereby declare that this submission is my own work and that, to the best of my knowledge and belief, it contains no material previously published or written by another person, except where due acknowledgement has been made in the text. In accordance with academic rules and ethical conduct, I have fully cited and referenced all material and results that are not original to this work. I am well aware of the fact that, on the basis of Article 36 Paragraph 1 Letter o of the University Law of 5 September 1996, the Senate is entitled to deny the title awarded on the basis of this work if proven otherwise.

Bern, Novemer 8, 2013